CHALMERS

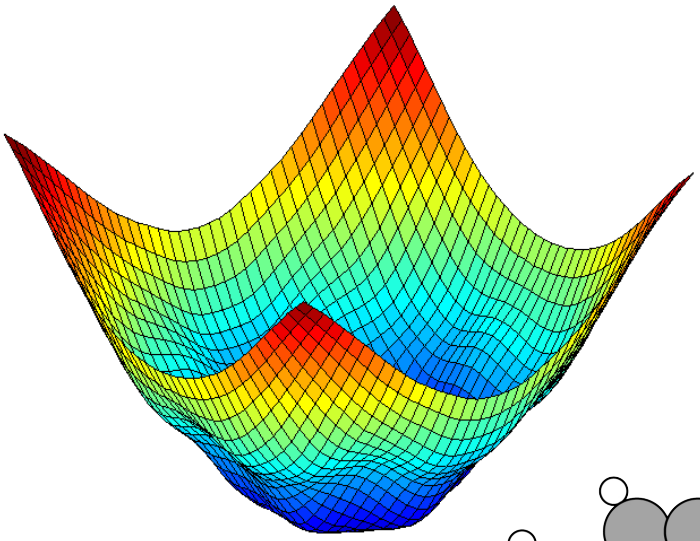

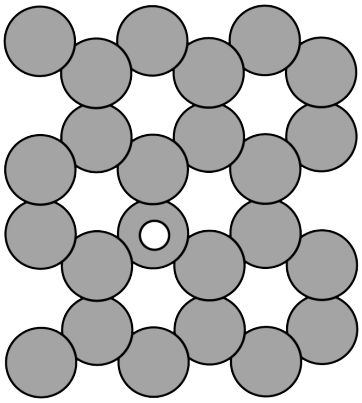

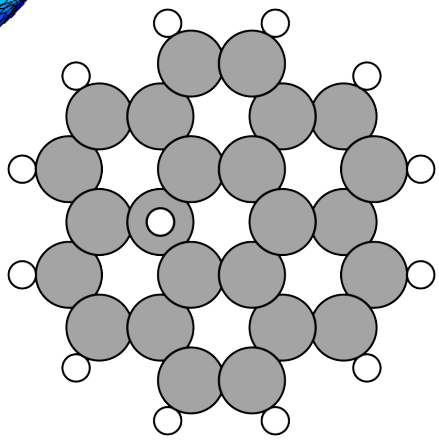

# Hydrogen adsorption on graphene and coronene

## A van der Waals density functional study

*Master of Science Thesis in Fundamental Physics*


ESKIL VARENIUS

Supervisor: Per Hyldgaard

Department of Microtechnology and Nanoscience, MC2

*BioNanoSystems Laboratory, Materials Physics and Carbon engineering group*

CHALMERS UNIVERSITY OF TECHNOLOGY

Göteborg, Sweden 2011

Thesis for the degree of Master of Science in Fundamental Physics

# Hydrogen adsorption on graphene and coronene

## A van der Waals density functional study

Eskil Varenius

Department of Microtechnology and Nanoscience, MC2
*BioNanoSystems Laboratory, Material Physics and Carbon engineering group*
CHALMERS UNIVERSITY OF TECHNOLOGY
Göteborg, Sweden 2011

**Hydrogen adsorption on graphene and coronene**
**A van der Waals density functional study**
Eskil Varenius

Thesis for the degree of Master of Science in Fundamental Physics



Department of Microtechnology and Nanoscience, MC2
BioNanoSystems Laboratory
Materials Physics and Carbon engineering group
CHALMERS UNIVERSITY OF TECHNOLOGY
SE-412 96 Göteborg
Sweden www.chalmers.se Tel. +46-(0)31 772 1000

**Cover:** *Top left* shows the binding energy calculated for a single hydrogen atom placed 2.85 Å above the surface of a coronene molecule. *Top right* shows a hydrogen atom at the Top site above a graphene layer. *Bottom* shows a hydrogen atom at the Top site above a coronene molecule.

Printed by Reproservice
Göteborg, Sweden 2011

# Hydrogen adsorption on graphene and coronene
A van der Waals density functional study

Eskil Varenius
*Department of Microtechnology and Nanoscience*
*Chalmers University of Technology*

**Abstract**
This thesis investigates hydrogen adsorption on graphene and coronene within the framework of density functional theory. The new nonlocal van der Waals density functional (vdW-DF) method is used: the original version, vdW-DF1, and the new higher accuracy version, vdW-DF2. Hydrogen adsorption is studied in the context of formation of molecular hydrogen in interstellar space, a process thought to depend on hydrogen adsorbing on a graphitic surface.

Calculations were done for hydrogen above coronene and graphene with both vdW-DF1 and vdW-DF2 to investigate how these functionals perform in the case of hydrogen adsorption on a graphitic surface. All calculations were performed with the software GPAW in a non-self consistent way based on underlying self-consistent GGA (revPBE) calculations.

The results show that vdW-DF2 predicts hydrogen to physisorb on a graphitic surface with an essentially site independent adsorption energy of ≈70 meV at a distance of 2.85-3.0 Å from the surface. The physisorption energy is overestimated by 30 meV compared to experiment and accurate quantum chemical studies, but the binding distance is in good agreement. The functional vdW-DF1 gives around the same adsorption energy and adsorption distance. In the case of physisorption coronene seems to be a good model of graphene, provided the adsorption sites are in the vicinity of the innermost carbon ring.

The results also show a barrier between the chemisorption and physisorption wells of up to 597 meV, which is high. However, this result was obtained in the absence of relaxations in the vdW-DF2 study. Atomic relaxations affect the chemisorption behaviour and energies and I expect that the barrier will be significantly lower in calculations which includes the chemisorption-induced morphology changes of the coronene or graphene substrates.

In the barrier region it was also hard to make the calculations converge due to partial spin-polarisation of the system. With tougher limits for convergence in the barrier region it is possible that the height will be lower.

The calculations performed in this thesis indicate that it is important to use a spin-polarised description of the physics to get accurate results for hydrogen adsorption on a graphitic surface.

**Keywords:** DFT, van der Waals, vdW-DF, hydrogen, coronene, graphene, physisorption.

## Acknowledgements

I want to express deep gratitude to my supervisor Per Hyldgaard for his everlasting enthusiasm and for all good ideas. It is a pleasure to work with you!

I also thank Elsebeth Schröder, Bengt Lundqvist, André Kelkkanen, Jochen Rohrer, Kristian Berland, Elisa Londreo and Peder Olesen for very good advice and a lot of fun discussions. An extra thanks to Gerald D. Mahan who shared interesting ideas about van der Waals forces during his six weeks stay at Chalmers.

A special thanks go to Mattias Slabanja and Thomas Svedberg at C3SE support for excellent support and valuable assistance during my work with the Beda cluster.

I also want to thank Alexander Tielens, Kay Justtanont, John Black and René Liseau for helping me with finding information about molecular hydrogen formation in space.

Finally I want to thank Magnus Sandén for beeing a very good friend, for fascinating discussions and for sharing his endless programming wisdom.

Göteborg, June 2011
Eskil Varenius

# Contents

# Chapter 1

# Introduction

Quantum physics has opened strong connections between seemingly different areas of science. The development of computers and computer science today makes it possible to use the models of physics to accurately calculate what happens in chemical reactions. This kind of meeting ground for phenomena in chemistry, biology and physics bodes for very interesting times around the corner. One may, for example, consider the potential for a new computational theory of biology. Accurate simulations of DNA (see figure 1.1(a)) and other large molecules important in biology is right now starting to show promising results, and researchers use models based on quantum physics trying to calculate how viruses work.

What I personally find very interesting is the chemical process where hydrogen atoms in interstellar space combine to form molecular hydrogen and more complex molecules. Hydrogen is the most abundant element in the universe. Because of its abundance molecular hydrogen ($H_2$) can dominate the spectral characteristics of molecular clouds [1]. Clouds of molecular hydrogen are often associated with star formation regions such the famous Eagle nebula, figure 1.1(b).

Astrophysicists believe that the formation of molecular hydrogen happens on the surface of graphitic (graphite like) grains [1]. To investigate this formation process one can use quantum physics simulations.

Much theoretical work has been carried out related to the formation process and various studies uses simulations based on quantum physics. Most of these quantum physics models are at some point incorporating empirical corrections. In this thesis I use a very recent non-empirical model to investigate the interaction of hydrogen with a graphitic surface. This work illustrates the current reach of the model, and how it can be used to understand problems where long range forces are important.

In this introductory chapter I give a brief overview of concepts central to the further chapters in this thesis. The first section contains an introduction to molecular hydrogen in interstellar space. In the second section I briefly discuss van der Waals forces and why they are interesting in this context. The third section contains a brief survey of earlier studies related to the formation of molecular hydrogen in interstellar space. Finally, in the last section I describe the purpose of this thesis and provide a brief overview of the remaining chapters.

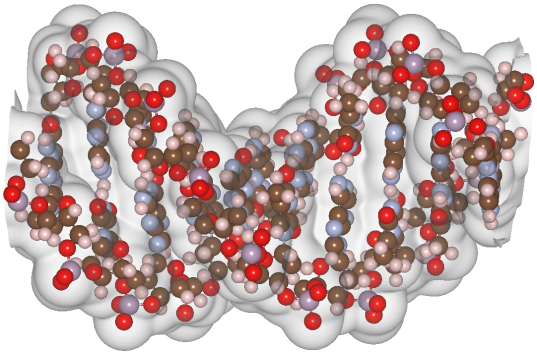

(a) Electron density of DNA.

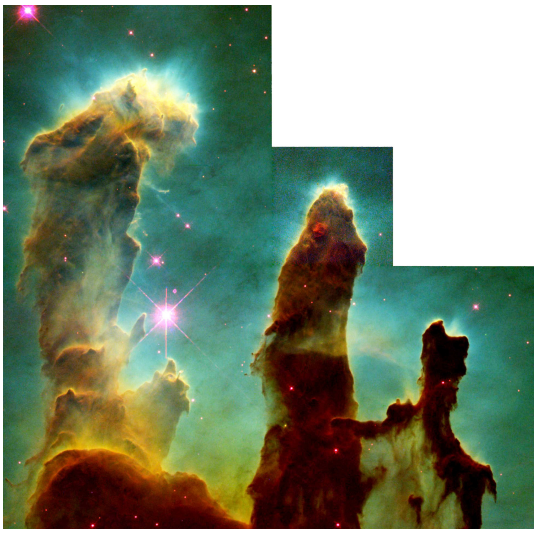

(b) The eagle nebula.

(c) A gecko climbing a wall.

Figure 1.1: Expressions of van der Waals binding. Panel (a) shows the ground state electron density for 700 atoms in DNA. Calculated with LCAO in GPAW by Eskil Varenius, Magnus Sandén and Elisa Londreo, spring 2011. Picture made using VESTA [2]. Panel (b) shows star forming pillars in the Eagle Nebula, as seen by the Hubble Space Telescope's WFPC2. Hydrogen physisorption on graphite is believed to catalyse a very high $H_2$ concentration in these clouds. Picture from Wikimedia Commons. Created by NASA (Public license). Panel (c) shows a gecko climbing on a glass surface. The millions of tiny hairs on the feet of the gecko get very close to the surface. The van der Waals forces between the hairs and the surface is thought to enable the gecko to adhere to smooth vertical surfaces [3]. Picture from Wikipedia Creative Commons, CCAS 3.0, GFDL License.

## 1.1 Molecular hydrogen in interstellar space

The obvious way of forming molecular hydrogen, $H_2$, is by taking two hydrogen atoms and putting them together. But in interstellar space the chance of two hydrogen atoms finding each other is not very big. In fact, calculations show (see for example chapter 8.7 in the book by A. Thielens [1]) that the process of forming molecular hydrogen through gas phase interactions between hydrogen atoms (or ions) is too slow to account for the observed formation rate. Therefore one might suspect that there is some other process causing the faster formation of molecular hydrogen.

### 1.1.1 The role of interstellar dust grains

It is today generally accepted within the astrophysics community that the formation of molecular hydrogen in interstellar space proceeds on the surfaces of interstellar dust grains (again chapter 8.7 in [1]). The basic idea is that one single hydrogen atoms have a much larger chance of finding a large grain structure than another single hydrogen atom. This means that suitable larger structures could catch many hydrogen atoms. These atoms may then move on the grain surface where they have a much higher probability of forming $H_2$ compared to free hydrogen atoms in a gas phase. In the diffuse interstellar medium the dominant grain surfaces are thought to be bare silicate (a compound containing silicon) and graphitic (graphite like) grains. The presence of graphite in the interstellar medium is supported by observations of a strong absorption of radiation with a wavelength around 200 nanometres. Graphite has a strong resonance around this wavelength and calculations show that the presence of graphitic grains of size around 30 to 200 Å would fit the observed feature very well, see the book by Thielens [1].

### 1.1.2 Two ways of forming $H_2$

Two ways of including interstellar grains in the process has been proposed. The first one is where two hydrogen atoms adsorb on a surface, move around and meet to form $H_2$. This process is called the Langmuir-Hinshelwood (LH) mechanism. The second one is where one hydrogen atom first adsorb at a fix site on a surface. A second atom outside the surface then combines directly with the atom already adsorbed and forms $H_2$. This is called the Eley-Rideal (ER) mechanism. Both these processes rely on the fact that one hydrogen atom is first adsorbed on the surface of a dust grain.

In the LH case the the atoms needs to be able to move around the surface. This suggests that the binding of hydrogen to the surface must be a weaker van der Waals bond, a physisorption well with very low corrugation (and a vanishing site preference). If there is a physisorption well it is also probable that atoms caught here might combine with atoms in the gas phase through the ER mechanism. It is central to study the physisorption (or van der Waals binding) of hydrogen atoms to a graphitic surface.

### 1.1.3 Applicability of computational studies

For the physisorption studies there is strong need to provide a physics based account of dispersive (vdW) interactions. The extreme computational cost of quantum chemical methods obviously affects the scope of system sizes in the computational studies. Theoretical investigations have often centred on the adsorption of hydrogen on poly-aromatic hydrocarbons (PAHs), for example the molecule coronene (see figure 1.2(c)) as a model for the graphene surface. For the physisorption of hydrogen on PAH molecules there have been previous theoretical studies using the far more efficient *density functional theory* (DFT) method, for example [4] see section 1.3. The advantages of DFT is that it can address extended systems like adsorption on graphene. Jacobson et al. [5] gives an example which also discusses inconsistencies that arise when using the old state-of-the-art approximations of DFT.

The traditional approximations used in the core of the DFT method assumed that a local or semi-local form was sufficient to approximate the correlations in electronic behaviour produced by many-body interactions. It is clear however that this procedures fails in the account of dispersive interactions which can act across regions with low or vanishing electron density, see [6] and [7]. This work takes off from a recent and successful formulation of a new standard approximation in DFT, the van der Waals density functional (vdW-DF) method which for example can describe the vdW binding and physisorption on both molecules and extended systems [7] like graphitic grains.

Since the spacing between the layers in graphite is large one may assume that calculations including a single graphene sheet (one layer in graphite) should give good results. Several computational studies have taken yet another step and used the molecule coronene ($C_{24}H_{12}$) as a model for the graphene surface. Pictures of these three models, graphite, graphene and coronene, can be seen in figure 1.2.

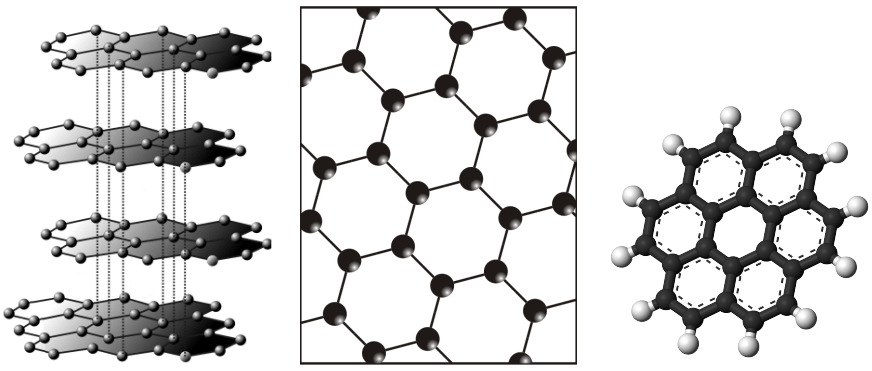

(a) Graphite (b) Graphene (c) Coronene

Figure 1.2: Three possible models of the surface of interstellar carbon grains. Figure (a) shows the layered structure of graphite (picture from Wikimedia Commons, CC BY-SA 2.5 license), figure (b) shows graphene i.e. one single layer from graphite (Picture from Wikimedia Commons, Public), and (c) shows the molecule coronene (picture from Wikimedia Commons, Public).

## 1.2 van der Waals forces

Atoms can bind together in different ways. What is meant by *van der Waals* forces varies in literature depending on the context. In this thesis the van der Waals forces refers to the forces which arise from long-range coupling of electrons. These are often also called London dispersion forces. This interaction is the principal interaction between inert atoms and molecules without permanent dipole moments. Their existence was first deduced by the investigation of inert gases by Johannes D. van der Waals in the late 19th century. For his work related to the van der Waals equation of state he was awarded the 1910 Nobel prize in physics. The reader further interested in Johannes van der Waals own views on his work may find his Nobel lecture [8] from 1910 interesting.

The van der Waals forces are attractive and relatively long ranged. In contrast to ionic bonds (which involves an electron transfer) and covalent bonds (which involves a lowering of total energy by sharing of electrons) van der Waals forces does not require any exchange of electrons between atoms. This means forces can arise between atoms over large distances. The strength of the van der Waals interaction is known to be proportional to $1/r^6$ for large separation distances $r$.

Since the forces arise over longer distances they, like gravity, increase with system size. Above extended systems like large surfaces the total force on an atom or a molecule can be comparatively large, even if the binding energy per atom is small. The Gecko is a famous example believed to make use of van der Waals forces to walk on walls or on a ceiling as in figure 1.1(c). Millions of tiny hairs cover the climbing tools that are the Gecko's feet. It is believed that when all these hairs come close to a surface the van der Waals forces becomes strong enough to make the Gecko stick to the surface [3].

### 1.2.1 The Lennard-Jones potential

The total potential energy of two rare-gas atoms or charge neutral molecules at separation $r$ is often written on an approximate form called the Lennard-Jones potential. This potential consists of two terms: one including attractive forces, and one including repulsive forces. The attractive term includes an account of approximate van der Waals forces described by the asymptotic $1/r^6$ behaviour. There are also repulsive forces that becomes important mainly for small distances. Experimental data on inert gases can be fitted well by an empirical potential proportional to $1/r^{12}$. The repulsive effect arise from the Pauli exclusion principle, the fact that electrons are fermions and cannot have all quantum numbers the same (see for example the book by Martin [21]).

The resulting expression for the Lennard-Jones potential is then (see [9] chapter 3)

$$V(r) = \frac{C_{12}}{r^{12}} - \frac{C_6}{r^6} \tag{1.1}$$

Other potentials are also used, although this nicely illustrates that both exchange effects (due to the Pauli exclusion principle) and correlation effects (such as van der Waals forces) are important.

The presented Lennard-Jones description also serves to introduce the semi empirical DFT-D method. In this type of computational scheme the empirical $C_6$ coefficient is included as an extra term to describe long-range interactions.

## 1.3 A brief survey of the field

The interest in hydrogen on graphitic surfaces has grown in recent years. As far as I know only one experimental investigation has been published, namely [10] done by Ghio et al in 1980. In this experiment the physisorption energy of a hydrogen atom on a graphite (0001) surface was measured to be $39.2 \pm 0.5$ meV. However, there are a lot of published computational studies investigating different properties of atomic and molecular hydrogen on graphitic surfaces.

This thesis is focused around my application of and calculations by the van der Waals density functional method. This is a new possibility for which the first paper only came out this spring, while I was working with this thesis. To complete the picture and provide the background this brief summary will focus on the work that has been published concerning hydrogen on graphitic surfaces where one have tried to account for van der Waals forces in some way.

### 1.3.1 Computational studies

The first study using density functional theory to investigate the formation of molecular hydrogen appears to be the work by Jeloaica and Sidis in 1999 [4]. The idea was to investigate the binding of hydrogen to a graphite-like surface. The molecule coronene ($C_{24}H_{12}$) was used as a model for a single layer of the dust grain graphitic surface. The calculations show that hydrogen prefer to physisorb directly above a carbon atom with an adsorption energy of 74 meV. Also, if the closest surface carbon atom is allowed to relax, a chemisorption well is found around 1.5 Å with adsorption energy of 600 meV. Between the chemisorption well and the physisorption well a barrier of height $\approx$200 meV is found. This study [4] by Sidis et al uses the Local Density Approximation (LDA) to calculate densities and they do also include added corrections calculated in the Generalised Gradient Approximation (GGA). However, the LDA has no genuine van der Waals component but is known to erroneously predict physisorption wells (also commented on by Sidis et al). The study acknowledges that the approximations used (the LDA as well as the GGA) do not describe van der Waals forces. There exists a number of related articles following this one (e.g. the study by Sha and Jackson from 2002 [11]) but neither of them try to describe the van der Waals forces.

There exists, to my knowledge, four published computational studies trying to include van der Waals forces in DFT. The first by Bonfanti et al from 2007 [12] observes that the old standard DFT methods are unreliable in describing van der Waals forces. Lacking a physics based account of van der Waals interactions instead standard quantum chemical methods are used to investigate the physisorption binding energy of hydrogen on a graphitic surface. The surface was also here modelled as a coronene molecule. The calculations predict hydrogen to adsorb above the middle of a carbon ring with an adsorption energy of 39.7 meV at a distance of 2.9 Å from the coronene surface.

The second van der Waals related study was performed by Psofogiannakis and Froudakis in 2009 [13]. The semi-empirical DFT-D method is used, where a correction term is added to model dispersion forces. The dispersion corrections were of the type proposed by Grimme [14] and [15]. The graphitic surface is modelled as a coronene molecule. They find that the preferred physisorption site for hydrogen on coronene is the hollow site (above the middle of a carbon

ring). This site has a physisorption energy of 30.4 meV at a distance of 3 Å from the coronene surface. A chemisorption well was also found with an adsorption energy of 720 meV at a distance of 1.1 Å from the coronene surface.

The third van der Waals related DFT study is by Ferullo et al from October 2010 [16]. They summarise earlier non-vdW studies [4], [11], [12] and [13] as that hydrogen can bind through chemisorption with an adsorption energy of about 800 meV or through physisorption with adsorption energy of about 40 meV. Between these two wells there is a barrier of around 200 meV. The investigation by Ferullo et al also uses the coronene molecule as a model for the graphitic grains. Here one includes van der Waals interactions through the addition of a semi-empirical correction to the total energy calculated in the PW91 [17] version of GGA. They find that the preferred physisorption site for hydrogen on coronene is the hollow site (above the middle of a carbon benzene ring). This site has an adsorption energy of 38.1 meV at a distance of 2.81 Å from the coronene surface.

The fourth and most recent study is by Jie Ma et al from April 2011 [18]. This article was published during the final stage of this thesis work. In [18] calculations were performed both on a coronene molecule and on a graphene surface. Several different computational techniques were compared, amongst them the first version of the van der Waals density functional (vdW-DF) method that has been developed within a long-standing Chalmers-Rutger collaboration. The calculations for vdW-DF1 were performed using the software VASP with an implementation of the PAW method. This recent study and my investigation supports each other. It is very interesting to compare the results in this thesis obtained using the code GPAW with those obtained using the code VASP in [18] and see how the results of different codes compare.

The VASP calculations with vdW-DF1 in [18] show that hydrogen is physisorbed with an adsorption energy of 75 meV at a distance of 3.0 Å from the coronene surface. In [18] it is also predicted that vdW-DF1 overestimates the binding energy by around 30 meV compared to accurate quantum chemical calculations (done with second order Møller–Plesset Pertubation theory, often abbreviated MP2). With a graphene surface the vdW-DF1 calculations show physisorption with an adsorption energy of 81 meV at a distance of around 3.0 Å from the graphene surface.

My present investigation provides an accurate description of the hydrogen physisorption as described in both the first and second version of the vdW-DF method. It was performed independently of [18]. Unlike [18] my study presents a first discussion of the role of spin in the calculations.

## 1.4 Purpose and overview

In this work I focus on the problem of H and $H_2$ interactions with a graphite-like surface using the vdW-DF method, a new framework for non-local density functional approximations. Theoretical simulations using density functional theory have in almost all previous cases either neglected the van der Waals interaction or employed a semi-empirical approach which does not include effects of adsorption inducing a charge transfer.

Recent publications (see the brief survey; section 1.3) show promising results for physisorption energy and physisorption distance which are in excellent agreement with the single experiment that I am aware of [10]. However, none of them (except for the recently published study by Jie Ma et al [18]) use a pure first-principle density functional theory approach. In the recent years a group at Chalmers have developed such a density functional with the ambition of describing van der Waals forces in a better way without the need of empirical corrections. This so called *van der Waals density functional* (or vdW-DF1 for short) was first developed in 2004. A second version of the functional was proposed in 2010 and called vdW-DF2 for short.

The purpose of thesis is to investigate how both versions of the so called *van der Waals density functional* perform when describing hydrogen adsorption on graphene and coronene. As far as I know there has been no calculation (except Jie Ma et al [18]) using a pure first-principle density functional trying to include van der Waals forces in the studies of hydrogen - graphite binding and Jie Ma et al [18] only use the first version vdW-DF1. It is therefore of interest to compare the results for vdW-DF1 and vdW-DF2 with results from other related studies mentioned in section 1.3. Finally this thesis also contains a first discussion on the role of spin in the transition region between chemisorption and physisorption configurations.

The rest of this thesis is organised as follows. Chapter two describes the underlying theory of density functional theory (DFT) and the van der Waals density functional. Chapter three describes the calculations done in this work; the hardware, the software and the atomic systems and related topics. Chapter four contains the results and a discussion of the results in relation to other related studies. The final chapter contains a short summary and an outlook.

# Chapter 2

# Theory

This chapter provides a brief theoretical background for the methods used in this thesis. The focus is on *density functional theory* (DFT) and different concepts related to the practical use of DFT. A brief description of the *van der Waals density functional* (vdW-DF) method and *the projector augmented wave* (PAW) method is also included. Formulae are written in Hartree atomic units ($\hbar = m_e = e = 4\pi/\epsilon_0 = 1$) if not stated otherwise.

## 2.1 Density functional theory

The problem of calculating properties for a piece of material can in many cases be reduced to the problem of calculating properties of the electrons in the material. To get accurate results one needs to consider that electrons live in the world of quantum mechanics. Hence the problem is: solve the Schrödinger equation for the system. Unfortunately the Schrödinger equation cannot be solved analytically except for a single hydrogen atom.

Naturally one tries to solve the equation numerically with help of computers. But, the full many-particle wave function is a very complicated thing. (For a description of exactly how complicated, see for example the book by Fetter and Walecka [19]). The complexity grows very badly with system size, and therefore solving the full many-particle wave function directly is too hard (even with numerical methods except for very simple model systems with very few electrons). It simply takes too much time and too much memory, thus for relevant materials problems it is impossible. But if we are satisfied with knowing the electronic structure (i.e. we do not care about other special properties of the wave function) then we do not really need the full many-particle wave function. In fact, the electronic structure can be described by a much simpler quantity: the electron density in space.

The density only requires one value for each point in space regardless of the number of particles involved. This is computationally much simpler to represent compared to the full many-body wave function. This is the idea of density functional theory: to reformulate the many-particle problem into another problem in terms of the electronic density.

Density functional theory is based on two theorems first proved by Hohenberg and Kohn in 1964 [20]. Loosely speaking these theorems state that it is

possible to express the energy of an interacting many-body system as a functional of the density, and that all properties of the system are completely determined from only the ground state density. Later, Levy and Lieb came up with a more general formulation of DFT which amongst other things makes the theory valid also for degenerate ground states. For a detailed discussion of differences between the Hohenberg-Kohn and Levy-Lieb formulations see for example [21] chapter 6. In this section I want to show one way of deriving the expression for the energy in terms of a universal functional. Since I find the Levy-Lieb formulation more clarifying and intuitive I follow their reasoning here, as outlined in [21].

It is helpful to first point our a number of choices that I have made in my presentation. In DFT the *Born-Oppenheimer approximation* is used, i.e. the atomic nuclei are fixed and can be treated classically. The classical Coulomb interaction between the nuclei is included in DFT. However, I chose to not include the term describing the nuclei-nuclei interaction, it is easily added to the final expressions. Note also that the Hamiltonian obviously depends on spin (and spin is sometimes important), but I have dropped the spin dependence in this brief derivation to make the expressions clearer. A further discussion about spin-dependent DFT is left to section 2.4.

### 2.1.1 The universal energy functional

To describe the quantum mechanical system completely it is sufficient to know the Schrödinger equation for the system. The complete many particle Schrödinger equation for a non-relativistic system can be written in compact form by use of Dirac's bra-ket notation as

$$\hat{H}\left|\psi\right\rangle = \epsilon\left|\psi\right\rangle \tag{2.1}$$

where the Hamiltonian operator $\hat{H}$ is defined as

$$\hat{H} = \hat{T} + \hat{V}_{\text{int}} + V_{\text{ext}}(\mathbf{r}) \tag{2.2}$$

The three terms in $\hat{H}$ represent *kinetic energy*, *potential energy due to internal forces*, and *potential energy due to external forces*. From quantum mechanics we know that the density is defined in terms of the wave functions as

$$n(\mathbf{r}) = |\psi(\mathbf{r})|^2 \tag{2.3}$$

and the total energy for a system in the state $\psi$ can be written

$$E = \left\langle\psi\right|\hat{H}\left|\psi\right\rangle = \langle\psi|\hat{T}|\psi\rangle + \langle\psi|\hat{V}_{\text{int}}|\psi\rangle + \int d^3r V_{\text{ext}}(\mathbf{r})n(\mathbf{r}) \tag{2.4}$$

The energy of the ground state can, in principle, be found by minimising the expression for the total energy with respect to all possible states $|\psi\rangle$. But suppose that one first minimises the energy only for the set of states $|\psi\rangle$ *having the same density* $n(\mathbf{r})$. In this case we can write the lowest energy for that density as a functional (i.e. a function of a function, in this case a function of the density)

$$\begin{aligned} E[n] &= \min_{\psi\to n(\mathbf{r})}\left[\langle\psi|\hat{T}|\psi\rangle + \langle\psi|\hat{V}_{\text{int}}|\psi\rangle\right] + \int d^3r V_{\text{ext}}(\mathbf{r})n(\mathbf{r}) \\ &\equiv F[n] + \int d^3r V_{ext}(\mathbf{r})n(\mathbf{r}). \end{aligned} \tag{2.5}$$

If we know the external potential $V_{\text{ext}}$ and the *universal functional* $F[n]$, then 2.5 gives us the minimum energy *for a specific density* $n(\mathbf{r})$. To obtain the ground state energy of the system we must also minimise 2.5 with respect to all possible densities $n(\mathbf{r})$. The functional $F[n]$ is independent of the external potential $V_{\text{ext}}$.

The central question is now: what is the universal functional $F[n]$? There is no easy answer to this question, because finding an explicit expression for $F[n]$ corresponds to solving the full many-particle Schrödinger equation. Because of this, density functional theory might have remained a mere curiosity were it not for the approach taken by Kohn and Sham.

### 2.1.2 The Kohn-Sham approach

In 1965 Kohn and Sham [22] proposed a way to attack the problem of finding an expression for the unknown universal functional $F[n]$. It is obvious that each electron have kinetic energy, and also energy due to classical Coulomb repulsion between all electrons, but it is not possible to state exact expressions for these quantities because of complicated many-body effects. However, the kinetic energy and Coulomb energy must contribute to the internal energy of the system, and $F[n]$ should incorporate these quantities in some way.

It is not easy to see how the quantum mechanical many-body effects (exchange and correlation) affect the energy. Kohn and Sham thought that the complicated many-body effects of the interacting system (contained in $F[n]$) can be seen as a small correction to the total energy of a similar auxiliary system without difficult many-body effects. Therefore in the Kohn-Sham approach one replaces the original interacting system with a similar system that can be solved more easily. This simpler auxiliary system is chosen to have the same number of electrons as the original system, and it also has the same external potential.

Each single electron has a single-particle kinetic energy (free from many-body effects), and it also feels the Coulomb repulsion from all other electrons. So the Hamiltonian of this auxiliary system must consist of *the kinetic energy*, *the classical Hartree energy* and *the external potential*. Using the DFT formalism we can rewrite the expression for the ground state energy of the auxiliary system as functional of the density

$$E_{\text{aux}}[n] = T_s[n] + E_{\text{Hartree}}[n] + \int d^3r V_{ext}(\mathbf{r}) n(\mathbf{r}). \tag{2.6}$$

The first two terms here can be calculated provided that one knows the one-electron wave functions $\phi_i$ of the auxiliary system as

$$\begin{aligned} T_s &= -\frac{1}{2}\sum_{i=1}^{N} \langle \phi_i | \nabla^2 | \phi_i \rangle \\ E_{\text{Hartree}} &= \frac{1}{2}\int d^3r d^3r' \frac{n(\mathbf{r})n'(\mathbf{r})}{|\mathbf{r}-\mathbf{r}'|} \\ n(\mathbf{r}) &= \sum_{i=1}^{N} |\phi_i|^2 \end{aligned}$$

Now, in the Kohn-Sham approach to DFT one *assumes* that the auxiliary system can be chosen to have the same ground state density as the original interacting system. To make this possible one must change the auxiliary system in some way to represent many-body effects that exist in the actual physical system. A new term must express the difference between the original and the auxiliary systems, and it must in the DFT formalism be defined as a functional of the density. Kohn and Sham called this extra term the *exchange-correlation functional*. All difficult many-body effects are incorporated in this *exchange-correlation functional* $E_{\text{xc}}[n]$. Formally this can be written in terms of an expression for the universal functional $F$ as

$$F[n] = T_s[n] + E_{\text{Hartree}}[n] + E_{\text{xc}}[n]. \tag{2.7}$$

The beauty of this procedure is that $E_{\text{xc}}[n]$ is also universal and can be evaluated - or realistically approximated (for example by many-body theories or from quantum Monte Carlo methods) - once and for all. If we can find an *exact* expression for the last term $E_{\text{xc}}[n]$ then we can actually calculate the *exact* energy of the original interacting system! The expression for the total energy becomes

$$E[n] = T_s[n] + E_{\text{Hartree}}[n] + \int dr^3 V_{\text{ext}}(\mathbf{r}) n(\mathbf{r}) + E_{\text{xc}}[n]. \tag{2.8}$$

Here $T_s$ is the kinetic energy of the independent particles, $E_{\text{Hartree}}$ is the self interaction energy of the (classical) electronic density and $E_{\text{xc}}$ is the exchange-correlation energy. Two problems must be solved before one may actually calculate physical properties of materials and systems.

One is to obtain the single-particle wave functions $\phi_i$ needed to construct the kinetic energy and the density of the auxiliary system. For any given nonzero exchange-correlation the original auxiliary Hamiltonian is no longer valid. Before one can obtain the single-particle wave functions the auxiliary Hamiltonian must be modified to incorporate the effect of the exchange-correlation term. To find this modification one may use the powerful tool of variational calculus. This is discussed further in section 2.1.3.

The other is to find an actual approximate expression for $E_{xc}$. It is not possible to find an exact expression, but there are many good approximate expressions available. This is discussed further in section 2.3.

### 2.1.3 The Kohn-Sham equation

The tool of variational calculus can be used to find an equation which solutions minimise the energy functional (equation 2.8). If one minimises with respect to the density one gets the so called Kohn-Sham equation. For the actual derivation I refer to standard textbooks, e.g. [21]. The resulting equation turns out to be a Schrödinger-like equation for the auxiliary system where the potential has an extra term due to exchange-correlation effects

$$H_{\text{eff}} |\phi_i\rangle = \left[ -\frac{\nabla^2}{2} + V_{\text{Hartree}}(\mathbf{r}) + V_{\text{ext}}(\mathbf{r}) + V_{\text{xc}}(\mathbf{r}) \right] |\phi_i\rangle = \epsilon_i |\phi_i\rangle \tag{2.9}$$

The solutions to this equation are the so called Kohn-Sham orbitals $\phi_i$ for the auxiliary system with the approximated many-body corrections present in the form of the exchange-correlation term.

## 2.2 Solving the Kohn-Sham equation

The Kohn-Sham equation is in practise solved numerically by an iterative procedure called the self-consistency loop. The procedure is as follows:

1. Make an initial guess for the electron density $n(\mathbf{r})$.
2. Construct the Kohn-Sham Hamiltonian based on this density.
3. Solve the Kohn-Sham equation to get the Kohn-Sham orbitals.
4. Construct a new density from the Kohn-Sham orbitals.
5. Calculate the total energy of the input and output densities using 2.8. If the difference between these two energies is smaller than some threshold then the final energy is taken as the ground state energy for the system. If the energy difference larger than the threshold go to step 6.
6. Add a little of this new density to the old one to get a new input density and go back to step 2.

Finding the best way to mix the new and old densities in step 6 is not trivial. There are several different techniques available. A detailed discussion is beyond the scope of this thesis and I refer the interested reader for example to [21] chapter 9.

### 2.2.1 Numerical problems with the Kohn-Sham equation

The basic result of density functional theory is that one may rewrite the problem of the many-particle Schrödinger equation in terms of a functional of the electronic density. Kohn and Sham then found a way to practically divide the functional into an exact (but incorrect) part describing an auxiliary system, and a correction part to account for the missing many-body effects. The equation governing the auxiliary system is called the Kohn-Sham equation and it describes independent electrons in an effective potential. The effective potential includes the (approximated) many-body effects of the system. This simplification is a great achievement, but the resulting Kohn-Sham equation is still difficult to solve numerically close to the atomic nuclei.

The reason is that in the region of space close to the atomic core the wave functions of the valence electrons oscillate very rapidly. This rapid oscillation happens because the valence states are required to be orthogonal to the core states. To represent these rapid oscillations with sufficient numerical accuracy a very fine grid is required. To use a fine enough grid in the whole space region is not computationally feasible, but since we want to do calculations anyway we need to find a way around this. In this thesis I use software based on one of several ways around this problem: *the projector augmented wave method*.

### 2.2.2 The projector augmented wave method

One way of treating the problem of rapidly oscillating wave functions is the so called *projector augmented wave method* or PAW for short. In short the PAW method uses a coarse grid for the region between atoms in a system, and a finer grid in the close vicinity around each atomic core. The PAW method was

presented by P. E. Blöchl in 1994 [23] and has been implemented several times since, for example in the softwares GPAW and VASP. All calculations in this thesis were performed with the PAW implementation GPAW (see section 3.2). The key reason for choosing GPAW was that the *van der Waals functional* is implemented and ready to be used with GPAW. I also wanted to learn more about the PAW method, and GPAW seemed like a comparatively user friendly implementation. In the following section I will very briefly discuss the basic ideas behind the PAW method.

### 2.2.3 Creating a PAW model of an atom

The basic assumption in the PAW method is that the innermost bound electrons are not affected by atomic interactions such as chemical bonding. Thus one may treat the inner (core) and outer (valence) electrons differently. When doing calculations with the PAW method one actually does calculations not on real atomic configurations, but on models that are very similar in a well defined way. When creating these atomic models one uses the assumed differences between the core and the valence electrons. The major concepts of the PAW method are all present in the creation of these atomic models (called atomic setups in GPAW). Therefore I find it convenient to explain the PAW method in terms of how to create such an atomic setup. One may divide the process of creating an atomic setup into three broad steps.

The first step is to define an *augmentation sphere* around the atomic core. The radius of the augmentation sphere is chosen so that the problematic parts of the valence electron wave functions are inside the sphere. This means that the sphere cannot be too small. But, inside the sphere we want to be able to represent the wave functions in a local basis of atomic orbitals. This means that the sphere cannot be too big, because far out the wave functions cannot be well represented in a basis of atomic orbitals. In practise one has to check carefully so that the choice of radius works well for all calculations of interest.

The second step is to *freeze the core-electrons* so they are not allowed to change during calculations. This restriction may in principle be lifted but is imposed for various reasons [23]. The core state information is used to calculate a core electron density (and to restrict the basis set of the valence functions to a set orthogonal to the core states). This is only done once, after the creation of an atomic setup the core states will not change during DFT calculations.

The third step is a *transformation of the valence states*. Far from the atomic cores the valence wave functions are smooth and a course grid gives good results. Close to the atomic core the electronic wave functions can be well represented (locally) in a basis of atomic orbitals. The projection of valence states onto atomic orbitals is done with help of so called *projector functions*. When the valence states are represented in atomic orbitals we may do a change of basis to another more convenient locally good basis in which one gets smooth wave functions close to the atomic core. This change of basis defines a transformation of the valence states.

The calculations can now be done on smooth functions both close to the atomic core and far away from the core. Note the difference compared to the core states: The valence states are allowed to relax everywhere (also in the core-region) during the calculation. But even though the valence states change during the calculation, the basis sets will not change. Therefore the transformation will

continue to be valid during all iterations. However, as in the case of the core charge density, the transformation will be different for different elements.

If one had to transform back and forth between the different basis sets at every iteration the PAW method would not be good at all. But it turns out that the PAW method allows for solving the Kohn-Sham equations iteratively without the need of transforming back to the true wave functions. When the solution has converged one may use the transformation to return to the true wave function in all of space if desirable. The important point here is that the true wave functions are not needed to calculate the wanted electronic density. This means that we may solve the Kohn-Sham equations in a computationally efficient way.

A more detailed discussion of the PAW method is beyond the scope of this thesis. There is (of course) a lot more to learn about the PAW method for the interested reader. The original article by Blöchl from 1994 [23] contains a lot of information but can be hard to digest. For a detailed discussion of the theory behind the PAW method I recommend reading the masters thesis of Ask Hjort Larsen [24].

## 2.3 The exchange correlation functional

One practical way to interpret this term is as the difference in energy between the simple auxiliary system and the full interacting system. It includes exchange effects of the Pauli-exclusion principle as well as other correlated corrections. It is not feasible to find an exact expression for the term $E_{xc}$ because it would again correspond to solving the full many-particle problem. But, it is reasonable to assume that this term is small and therefore a good enough approximation could work. This is indeed the case and numerous such approximations have been developed. Much of the theoretical work within DFT has been about finding better and better approximations for the term $E_{xc}$ under the condition that the expressions must be computationally efficient.

### 2.3.1 The Local Density Approximation (LDA)

The first approximation for the exchange-correlation energy was proposed by Kohn and Sham in the same paper [22] as the so called Kohn-Sham approach described above. In this approximation, called the local density approximation (LDA), one assumes that the exchange-correlation effects are the same as in a system of a homogeneous electron gas. In LDA the effects of exchange and correlation are local in character and the exchange correlation term is

$$E_{\mathrm{xc}}^{\mathrm{LDA}} = \int d\mathbf{r} n(\mathbf{r}) \epsilon_{\mathrm{xc}}^{\mathrm{LDA}}(n(\mathbf{r}))$$

where $\epsilon_{\mathrm{xc}}^{\mathrm{LDA}}$ is the exchange-correlation energy per electron of a homogeneous electron gas at density $n$. This simple approximation works astonishingly well and gives good results for a lot of atomic systems. Further discussion of the LDA (and the spin-dependent version LSDA) is beyond the scope of this thesis and I refer the interested reader to standard textbooks, for example [21].

### 2.3.2 The Generalised-Gradient Approximation (GGA)

Following the success of the LDA many generalised-gradient approximations (GGAs) has been developed. Such an approximation is a functional not only of the density, but also of the magnitude of the gradient of the density $|\nabla n|$. GGA functionals are chosen to be on the general form

$$E_{\rm xc}^{\rm GGA} = \int d\mathbf{r} \epsilon_{\rm xc}^{\rm LDA} F(n, |\nabla n|, ...).$$

$F$ is called the *enhancement factor* and numerous forms have been proposed. In this thesis a GGA functional called *revised PBE* (or revPBE for short) [25] has been used for all self-consistent calculations. Further discussion of GGA functionals is beyond the scope of this thesis and I refer the interested reader to standard textbooks, for example [21].

### 2.3.3 The van der Waals density functional method

In 2004 a new functional called vdW-DF or vdW-DF1 was proposed [6]. It is actually two things. It is a specific new non-local approximation for the exchange-correlation energy $\rm E_{xc}$. It is also a new framework (today called the vdW-DF method) for extending the reach of DFT by account of dispersive or vdW interactions. The advantage of the vdW-DF method is that it is physics or constraint based and that it treats vdW forces at the same electronic level as DFT treats other types of interactions (e.g. covalent, ionic, metallic and hydrogen bonds) This functional has proven to give promising results for a wide variety of systems, see for example the review article [7].

The total energy functional within the vdW-DF method is defined in terms of the Kohn-Sham scheme outlined in section 2.1.2:

$$E^{\text{vdW-DF}}[n] = T_S[n] + E_{\rm H}[n] + \int_{\mathbf{r}} V_{\rm ext}(\mathbf{r}) n(\mathbf{r}) + E_{\rm xc}^{\text{vdW-DF}} \tag{2.10}$$

This expression includes the standard Kohn-Sham expressions for the the kinetic energy of the auxiliary system $T_S$, the electrostatic energy of the system $E_{\rm H}$ and the interaction with an external potential $V_{\rm ext}$ (the atomic cores). What is different in vdW-DF (compared to traditional functionals such as LDA and GGA) is that the correlation part of the energy has a non-local dependence on the density. The full expression for the exchange-correlation energy uses the exchange part of a GGA functional and the correlation part of LDA but adds also a non-local correlation term.

$$E_{xc}^{\text{vdW-DF}} = E_c^{\rm LDA} + E_x^{\rm GGA} + E_c^{\rm nl} \tag{2.11}$$

The functional vdW-DF1 uses the GGA functional revPBE [25] for exchange.

One should keep in mind that the standard Kohn-Sham expression for the kinetic and electrostatic energy is also non-local. What is special about vdW-DF is that there is a non-local part *also in the expression for the correlation.*

The expression for the non-local correlation in vdW-DF takes the form of a six-dimensional integral

$$E_c^{\rm nl}[n] = \frac{1}{2} \int_{\mathbf{r}} \int_{\mathbf{r}'} n(\mathbf{r}) \phi(\mathbf{r}, \mathbf{r}') n(\mathbf{r}') \tag{2.12}$$

with an *interaction kernel* $\phi(\mathbf{r}, \mathbf{r}')$. In the asymptotic limit this kernel has the well known $1/r^6$ behaviour characteristic for van der Waals interaction. Now, what is the expression for this kernel function $\phi$? The kernel function can be expressed in the following way (see [6]):

$$\phi(\mathbf{r}, \mathbf{r}') = \frac{2me^4}{\pi^2} \int_0^\infty a^2 da \int_0^\infty b^2 db W(a,b) \times T\left(v(a), v(b), v'(a), v'(b)\right)$$

where

$$T(w,x,y,z) = \frac{1}{2}\left[\frac{1}{w+x} + \frac{1}{y+z}\right]\left[\frac{1}{(w+y)(x+z)} + \frac{1}{(w+z)(y+x)}\right]$$

and

$$\begin{aligned} W(a,b) = 2[&(3-a^2)b\cos b \sin a + (3-b^2)a\cos a \sin b \\ &+ (a^2+b^2-3)\sin a \sin b - 3ab\cos a \cos b]/a^3b^3 \end{aligned}$$

The quantities $v$ and $v'$ are defined as

$$v(y) = y^2/2h(y/d) \qquad \text{and} \qquad v'(y) = y^2/2h(y/d')$$

where

$$d = |\mathbf{r} - \mathbf{r}'|q_0(\mathbf{r}) \qquad \text{and} \qquad d' = |\mathbf{r} - \mathbf{r}'|q_0(\mathbf{r}')$$

where the parameter $q_0(\mathbf{r})$ is defined as

$$q_0(\mathbf{r}) = \frac{\epsilon_{\text{xc}}^0(\mathbf{r})}{\epsilon_{\text{x}}^{\text{LDA}}} k_F(\mathbf{r}). \tag{2.13}$$

This quantity $\epsilon_{\text{xc}}^0$ is defined as the LDA expression for exchange and correlation, but with a gradient correction term as

$$\epsilon_{\text{xc}}^0 \approx \epsilon_{\text{xc}}^{\text{LDA}} - \left[\frac{Z_{\text{ab}}}{9}\left(\frac{\nabla n}{2k_F n}\right)^2\right]. \tag{2.14}$$

The LDA exchange used in equation 2.13 is defined as

$$\epsilon_{\text{x}}^{\text{LDA}} = -3e^2 k_F/4\pi$$

where, finally, $k_F$ is defined as

$$k_F^3 = 3\pi^2 n.$$

The parameter $Z_{\text{ab}}$ introduced in equation 2.14 determines the contribution of the gradient correction term. This quantity is obtained from first principles and for the functional vdW-DF1 the value is $Z_{\text{ab}} = -0.8491$. In principle, $Z_{\text{ab}}$ is not a constant but rather a function of electronic density. For further details about this gradient contribution in vdW-DF see [26] appendix B (and references therein).

A derivation of kernel expressions is beyond the scope of this thesis. For the interested reader a summarised derivation can be seen in [6] and for a detailed derivation I recommend reading the licentiate thesis of Berland [27], chapter 3 and appendix A.

### 2.3.4 vdW-DF2: a higher accuracy van der Waals density functional

In 2010 a second version of the *van der Waals functional* was proposed [28]. This functional (abbreviated vdW-DF2) is of course interesting to use in this thesis because it aims to improve the description of van der Waals forces. Since vdW-DF2 is comparatively new it is also valuable to compare the results of this second version to the results of the original functional vdW-DF1.

The full expression for the exchange-correlation energy uses the exchange part of the functional PW86 (see [28] and references therein) instead of revPBE. The correlation part is still LDA and similarly to vdW-DF1 a non-local correlation term is added:

$$E_{xc}^{\text{vdW-DF2}} = E_c^{\text{LDA}} + E_x^{\text{PW86}} + E_c^{\text{nl}} \tag{2.15}$$

However, the non-local correlation term is different from vdW-DF1 in that vdW-DF2 has $Z_{\text{ab}} = -1.887$. In vdW-DF2 this value comes from a high-density (instead of slowly varying density) many-body study.

### 2.3.5 Non-self consistent calculations

It is possible to do what is usually called *non self-consistent calculations* with DFT. Here one converges the density self-consistently with respect to one functional, and then uses this density to calculate the energy with another functional. This is used for example in situations where one wants to do a full DFT calculation with a certain choice of exchange-correlation functional, but the calculations with this functional are hard to converge in a self-consistent way, or are too time consuming.

For example one may want to do a calculation for a system with the functional vdW-DF2. A self-consistent calculation with this functional is more demanding than a self-consistent calculation with, say, the revPBE functional. Now, the goal of a DFT calculation is to get the ground state energy. This one does by self-consistently iterating to find a density, see section 2.1.3. It has been shown that in many cases the converged density is quite similar regardless of whether one uses vdW-DF2 or revPBE. But, the ground state energy as a functional of this density will differ. Here one may do a *non self-consistent* vdW-DF2 calculation based on revPBE. The idea is to first make a self-consistent calculation with revPBE to get a density. This revPBE density is then used as input for the total energy expressions of the vdW-DF2 functional. The resulting energy is called a non self-consistent vdW-DF2 energy based on a revPBE density. This method have proven to provide good results [26] and will be used extensively in this thesis.

## 2.4 Spin density functional theory

So far I have not discussed how the quantum mechanical property of spin $\sigma$ enters the expressions derived within DFT. The ground state electron density for a physical system might be spin polarised, i.e. $n(\mathbf{r}, \sigma =\uparrow) \neq n(\mathbf{r}, \sigma =\downarrow)$. This must happen in a system with a finite and odd number of electrons [21], for example the hydrogen - coronene system used in this thesis. It may also happen in an extended system like H on graphene. For many systems (such as atoms with an even number of electrons) one does not need to keep track of the spin-polarisation and such *spin-paired calculations* is generally a bit faster. However, it is possible to rigorously generalise the arguments of DFT to include two types of densities, the particle density $n(\mathbf{r}) = n(\mathbf{r}, \uparrow) + n(\mathbf{r}, \downarrow)$ and the spin density $s_\sigma(\mathbf{r}) = n(\mathbf{r}, \uparrow) - n(\mathbf{r}, \downarrow)$. The expression for the total energy is modified to depend not only on the particle density but also on the spin density, see for example [21]. A more detailed discussion of the derivation is beyond the scope of this thesis. Spin dependent versions of several exchange-correlation functionals have been derived, for example the *local spin density approximation* (LSDA), a spin dependent version of the LDA approximation.

### 2.4.1 Spin polarised van der Waals calculations: an important assumption

Calculations with the vdW-DF method on systems which are guaranteed to be spin polarised (e.g. hydrogen - coronene) must be seen as a first step in a more systematic theory programme. No derivation of a spin-dependent form for the non-local correlation in the vdW-DF method exist at present [29].

In GPAW, vdW-DF1 and vdW-DF2 are implemented in the form $E_{\mathrm{xc}} = E_{\mathrm{x}}^{\mathrm{GGA}} + E_{\mathrm{c}}^{\mathrm{LDA}} + E_c^{\mathrm{nl}}$. When one asks for a spin-polarised calculation the spin-polarised parts are really $E_x$ and $E_c$. There are certainly spin-polarised expressions for these first two terms of exchange and correlation. The last term, $E_c^{\mathrm{nl}}$, is the principal term separating vdW-DF from other functionals. One could assume that the plasmon energy which enters in the non-local correlation part is spin-independent. This approach is what has, for now, been coded into GPAW although no formal discussion or argument has been presented.

One important question arises: if one did a proper spin-polarised derivation of the vdW-DF kernel function, would the resulting expression still be invariant under spin-polarisation? The only correct way to answer this question is of course to do the derivation. Unfortunately this is a project far beyond the scope of this thesis. Doing spin-paired calculations is no alternative, because it cannot be done for systems with an odd number of electrons like the hydrogen-coronene system.

In this thesis I have opted instead to illustrate the importance of spin (in treatment of physisorption). In this illustration I have to make an assumption of how the spin would affect the non-local correlation effects. Here I **assume** that including spin-polarisation also in the derivation of the van der Waals functionals will not change the final expression for the kernel function.

# Chapter 3

# Computational strategy and schemes

This chapter first gives a short overview of the hardware and software used for calculations in this thesis work. Thereafter follows a description of the systems investigated in this thesis, and the calculations performed.

## 3.1 Hardware: the Beda cluster

All calculations in this thesis work were performed on the *Beda* cluster at Chalmers University of Technology in Gothenburg, Sweden. The Beda cluster is maintained by the *Chalmers Centre for Computational Science and Engineering* (C3SE) which is one of six centres for scientific and technical computing in Sweden. C3SE is a part of the *Swedish National Infrastructure for Computing* (SNIC). The Beda cluster has 268 nodes, 2144 cores and about 7TB of RAM [30].

## 3.2 Software: ASE and GPAW

All calculations in this thesis work were performed with the software GPAW (see [31] and [32]) and ASE (see [33]). GPAW stands for *Grid-based Projector-Augmented Wave method* and is a python implementation of the PAW method. ASE stands for *Atomistic Simulation Environment* and is a very useful python framework developed closely together with GPAW. I will now briefly describe ASE and GPAW to explain the relationship between these two softwares and the underlying theory.

### 3.2.1 ASE

I want to emphasise that the Kohn-Sham approach to DFT is in principle exact and parameter free. By using the *Born-Oppenheimer approximation* we focus on solving the electron structure problem where the positions of the nuclei are input parameters. In principle one could write a text file with the coordinates

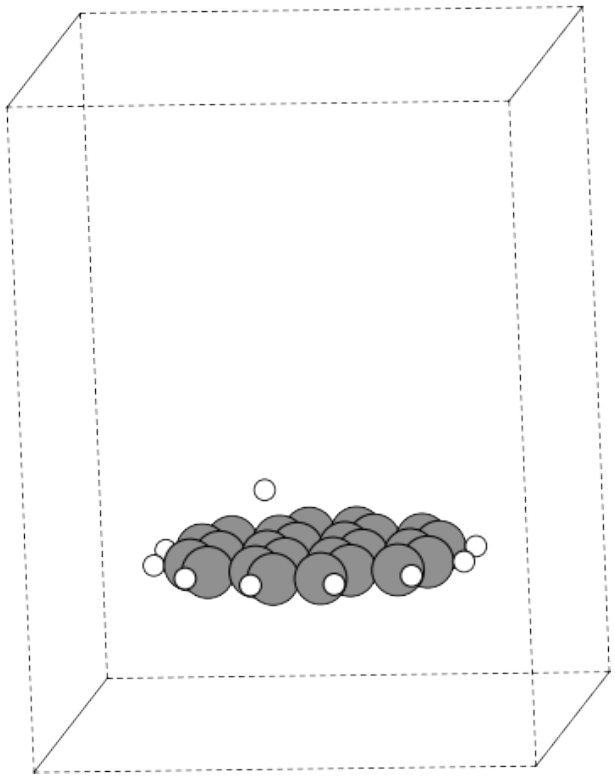

Figure 3.1: The hydrogen coronene system made with ASE. The hydrogen atom is here at a distance of 2.0 Å from the coronene surface.

of these nuclei and calculate the total energy with GPAW. However this is a very cumbersome way to do calculations.

The purpose of ASE is to make life easy when doing atomistic simulations with a calculator software like GPAW. Before using GPAW to calculate things one needs to set up the wanted atomic system in the computer. ASE handles the setup of atomic systems, and also external dynamics like relaxation using Hellman-Feynman forces (see section 3.3.3). ASE has support for a wide range of popular DFT-software codes like GPAW, DACAPO, SIESTA, VASP etc. I used ASE to put certain atoms inside a cell with a certain size, select boundary conditions and control the extent of atomic relaxation. As an example the hydrogen-coronene system I built with ASE can be seen in figure 3.1. When everything is set for a calculation one may attach GPAW (or some other software) to the atoms and ask for different physical quantities (like the total energy of the system).

### 3.2.2 GPAW

I again want to emphasise that the Kohn-Sham approach to DFT is in principle exact and parameter free. But the numerical implementation GPAW requires that the user makes certain choices. I will briefly describe these choices.

The first choice is whether one needs to do a spin-polarised calculation or not. As described in section 2.4 one may do either spin-paired or spin-polarised DFT. In my case I must use the spin-polarised DFT since the single hydrogen atom ground state cannot be described accurately in spin-paired DFT.

As mentioned in my brief description of the PAW method (section 2.2.2) one needs to create atomic setups for all elements in the calculation. The PAW method rests on the expansion of the wave function in local basis sets close to the atomic core. The choice of basis sets are made when creating the atomic setups, as described in 2.2.2. Such setups have been created and tested by the GPAW developers, and I used the latest official version 0.6.6300.

In the PAW method one also expands the valence wave functions on a sparse grid in the inter-atomic regions where bonding takes place. The specification of this grid is not included in the setup since the grid-spacing needed to achieve good results will depend on the atomic system. Therefore the grid-spacing must be specified when doing a GPAW calculation. I found that a grid spacing of 0.18 Å was enough to get converged results for my systems.

As described in section 2.1.3 the Kohn-Sham equations are solved in an iterative way. In GPAW there are several choices of eigensolvers available for solving the Kohn-Sham equation in an efficient way on the computer. The choice of eigensolver affects the number of iterations needed, and the stability of the convergence procedure. For the coronene calculations I used the *Conjugate Gradient* solver (or CG for short). For the graphene calculations I used the *Residual minimisation method - direct inversion in iterative subspace* (or RMM-DIIS for short).

As also described in section 2.1.3 one must set a threshold for when to consider the solution converged. This is in GPAW set in terms of a threshold for the total energy change between two iterations. I used a threshold of $10^{-6}$ eV/atom.

As described in section 2.1.3 one must also chose a good way of updating the density as described in section 2.1.3, so that the solution converges with in reasonable time. This is in GPAW implemented as a mixing parameter which determines how much to add of the new density. Most of the points were calculated with the default mixing of 0.1. In the barrier region for hydrogen on graphene some points were tricky to converge and there a mixing of 0.01 was used.

Another choice is to specify parameters for the Poisson solver used when calculating the Hartree energy part of the Kohn-Sham Hamiltonian. I set it to be more accurate than default in each iteration by specifying the parameter `eps=10`$^{-12}$.

Finally there are a couple of parameters that I did not change because the default choices worked fine. Instead of describing all default parameters here I chose to specify the version I used of ASE and GPAW for all calculations. This should, in addition to my explicit choices (described above) be sufficient information for anyone who wants to reproduce my results obtained using ASE and GPAW. For more information about the GPAW implementation see [31] and [32].

## 3.3 Calculation of binding energies

In this work ASE and GPAW have been used to calculate binding energies for different system configurations. When using DFT to calculate binding energies one always works with differences between total energies. The binding energy for a particular system is calculated as the difference between the total energy of the bound system and the total energy of the non-bound system. For example, the binding energy for a hydrogen atom at a certain distance $d$ from a coronene molecule is calculated as

$$E_{\text{binding}}(d) = E_{\text{Cor+H}}(d) - [E_{\text{Cor}} + E_{\text{H}}(d)] \tag{3.1}$$

So, to obtain the binding energy for a hydrogen atom at a certain distance one needs to do three separate calculations and combine them according to equation 3.1. As an illustration, hydrogen can be seen at a distance d above a graphene layer in figure 3.2.

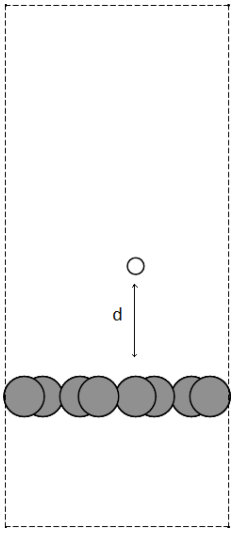


Figure 3.2: Hydrogen a distance d above graphene.

### 3.3.1 The reference energy for an isolated atom

In principle the reference energy of an isolated hydrogen atom ($E_{\text{H}}(d)$ in equation 3.1) should be independent of $d$, i.e. independent of where it is placed in the cell. But, since a finite set of grid points is used to represent the wave functions during calculations (and because of a finite convergence criteria) the energy might differ a little (around one meV) for the isolated atom depending on where it is. To correct for this I have calculated and used the reference energy for the isolated hydrogen atom at every $d$. The resulting binding energy calculated according to the distance dependent formula 3.1 is thus corrected for errors due to this distance dependence problem.

### 3.3.2 Binding energy as a function of distance

I wanted to find out the binding energy for H and $H_2$ as a function of the distance to some surface. This is easily done by calculating the binding energy (according to 3.1) for several distances. For each system I started by choosing a uniform distribution of points from 1.0 Å to 9.0 Å. The resulting values for the binding energy was plotted in Matlab as a function of distance. After inspecting the first plot I did additional calculations if needed to get more data points. This was done to get a finer resolution in regions of special interest. When I had obtained enough data points a final plot was made to illustrate the binding energy as a function of distance. Such a plot for the hydrogen - coronene system can be seen in figure 3.3.

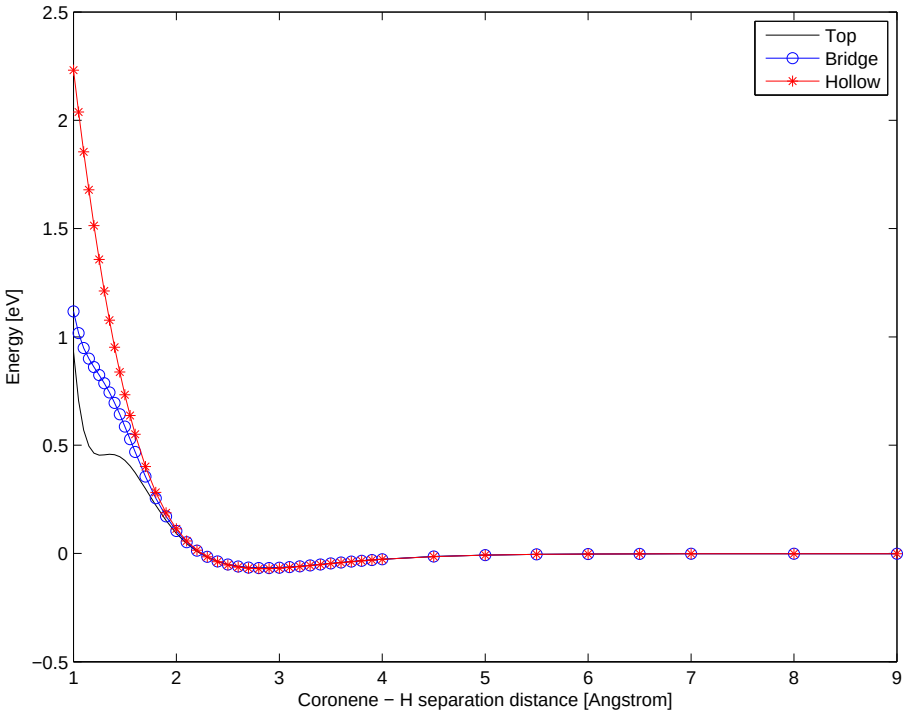


Figure 3.3: The binding energy of H - Coronene as a function of distance. This is a non-self consistent vdW-DF2 calculation based on an underlying self consistent revPBE calculation. No relaxation of atomic positions was allowed.

By inspection of this plot I could now get information about the chemisorption and physisorption regions. The important information to get was the position of minima, if they existed, and the value of the binding energy at the minima.

### 3.3.3 Surface relaxation

Earlier studies (e.g. [4]) indicate that the chemisorption well changes if the surface carbon atom closest to the hydrogen atom is allowed to relax. This is a more realistic calculation because in nature the system will of course relax to the lowest energy possible. To investigate the impact of relaxation the binding energy for the top site was calculated as in 3.4.2 but with relaxation. The relaxation was done with revPBE and the energies for vdW-DF1 and vdW-DF2 calculated non-self consistently using the relaxed electron density.

In a relaxation process the atoms move because of forces calculated from the total energy. But, in DFT the Born-Oppenheimer approximation is used which means the atoms are stationary - so how can they move? Well, the atoms doesn't move during a DFT calculation. But after finding the total energy of the system with atoms in certain positions it is possible to calculate the forces on the atoms using the derivative of the total energy with respect to atomic positions. When the forces are known it is possible to move the atoms a small distance according to the forces on each atom. This new atomic configuration can now be used as input for a new DFT calculation.

The calculation of forces rests on the *force theorem*, often also called the *Hellman-Feynman theorem* (see for example [21] chapter 3). In the naive application of the force theorem the nuclei moves relative to all electrons. However, in actual calculations it is more appropriate to move a part of the density (especially the core electrons) along with the nuclei. A more detailed discussion of forces is beyond the scope of this thesis, and I refer the interested reader to [21] chapters 3 and 9.

Relaxation is thus an iterative procedure where one iteration consists of finding the total energy with DFT, calculate the forces and then move the atoms a small distance. Some threshold is needed to stop this procedure, and usually the threshold is set in terms of the magnitude of the calculated forces. When the forces are smaller than some value the system is considered to have relaxed.

ASE supports several algorithms for structure optimisation. I used the Broyden–Fletcher–Goldfarb–Shanno (BFGS) algorithm and required the optimisation to run until the forces on all atoms were less than $0.0001\,\mathrm{eV/Å}$. In each step the total energy and forces were calculated using GPAW. The same versions and parameters were used as in the non-relaxed H-coronene case, see section 3.4.2. ASE also provides functions for fixing some atoms while relaxing others. To reduce the computational time required, and to be able to compare with similar studies e.g. [4] I kept all atoms fixed except the carbon atom closest to the adsorbed hydrogen atom.

### 3.3.4 Convergence with respect to k-points

Calculations of energies in programmes like GPAW are often performed with help of integrals in k-space (Fourier space). To evaluate integral expressions over the full k-space is very computationally demanding. In practise the integrals are approximated with a sum of values at special points. The number of points needed for the approximation to work well enough depends on the material. For many materials a good enough approximation can be obtained by using only one point. But for metals one usually needs more points. The number of

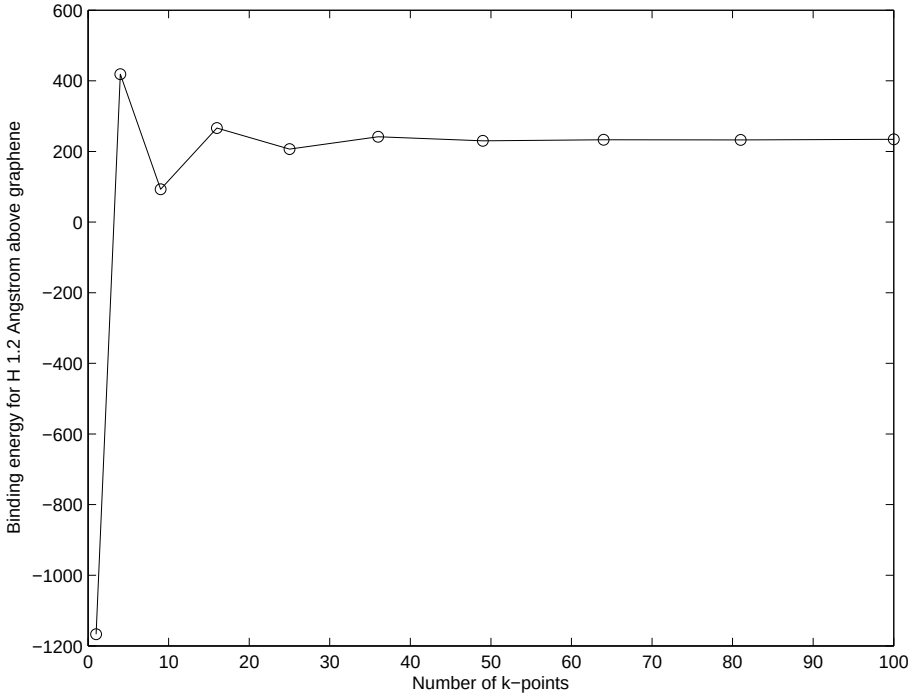


Figure 3.4: The binding energy of H - Graphene as a function of the number of k-points. This is a spin-polarised non-self consistent vdW-DF2 calculation based on revPBE. The hydrogen atom was placed at the vdW-DF2 chemisorption distance of 1.2 Å over the surface.

points is related to the cell size, so it is not possible to determine a number for a specific material. Using more points means the calculation takes longer to finish. Therefore it is desirable to know how many points are required to get a good result for the system under investigation. For the interested reader a more detailed discussion of integration over k-space using special points can be found in [21] section 4.6.

A practical way of determining the number needed for the setup with graphene used in this thesis is to plot the binding energy for one specific distance as a function of the number of k-points. The quest is to find the lowest number of k-points that gives a sufficient accuracy. Such a convergence test was carried out for the system H on graphene, and the results are assumed to be valid also for the calculations of $H_2$ on graphene in this thesis. The hydrogen atom was placed at the top site at a distance of 1.2 Å from the surface. The binding energy was calculated using different numbers of k-points: 1, 4, 9, 16, 25, 36, 49, 64, 81 and 100. The resulting convergence plot (using non-self consistent vdW-DF2 based on revPBE) can be seen in figure 3.4. The calculation was considered to be converged when using 64 or more points. In this thesis 64 points were used for all calculations with graphene.

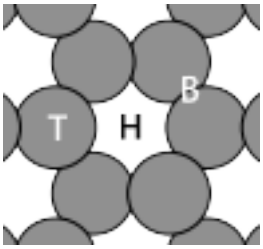


Figure 3.5: The three adsorption sites; Top (T), Bridge (B) and Hollow (H).

## 3.4 Atomic systems and adsorption sites

In this section I describe the coronene and graphene systems that I have used in calculations as models of a graphitic surface. I start with describing three adsorption sites and thereafter describe each atomic system in detail.

### 3.4.1 The Top, Bridge and Hollow sites

A graphitic surface has a regular pattern in the $x$ and $y$ directions. To investigate the binding energy as a function of $x, y$ position relative to the surface earlier studies have chosen a few different adsorption sites relative to the surface. For each of these sites the binding energy is calculated as a function of height over the surface (the separation distance $d$ in formula 3.1). I follow the approach used in [4] and use three sites: Top, Bridge and Hollow. The Top site is directly above a carbon atom, the Bridge site is above the middle point between two adjacent carbon atoms, and the Hollow site is above the middle of a carbon ring, see figure 3.5.

### 3.4.2 The H - Coronene system

Coronene ($C_{24}H_{12}$) is a planar molecule. In this thesis work the molecule was used as one model of a graphitic surface. Therefore the C-C bond length in the coronene molecule was kept at 1.42 Å. This value is used by ASE to create graphite and graphene structures. The C-H bond length was kept at 1.084 Å as done in previous studies e.g. [4]. The coronene molecule was constructed with help of ASE3 and placed together with a single hydrogen atom in a unit cell with non-periodic boundary conditions in all directions. The cell was a cuboid measuring $15 \times 15 \times 20$ Å in the $x \times y \times z$ directions. The coronene molecule was placed at a height of 5 Å so that the space above the coronene molecule was a cube with side 15 Å. The hydrogen atom was placed at different heights (different values of the $z$-coordinate) above the coronene molecule. For each site the binding energy was calculated according to equation 3.1. The coronene molecule with a hydrogen atom adsorbed at the Top position can be seen in figure 3.6.

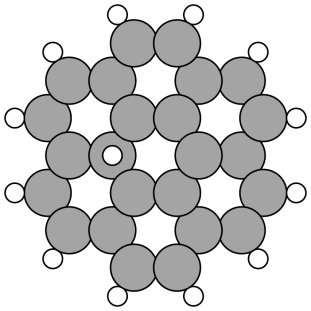

Figure 3.6: The coronene molecule used in calculations. Here a hydrogen atom is adsorbed at the Top site.

#### Versions and parameters

The H-coronene system was built using ASE 3.4.1.1765. The energies for vdW-DF1 and vdW-DF2 were calculated in a non-self consistent way based on revPBE, see section 2.3.5. The underlying self consistent revPBE calculation was a spin-polarised calculation performed using GPAW 0.7.2.6974. The calculator grid-spacing was specified as `h = 0.18`, the `eigensolver` was set to `cg` and convergence criteria `total energy change` was set to $10^{-6}$ eV/atom. The non-self consistent vdW-DF1 calculation was performed using GPAW 0.7.2.6974. The non-self consistent vdW-DF2 calculation was performed using GPAW development build r7883.

### 3.4.3 The H - Graphene system

Another model of a graphitic surface is a graphene sheet. A graphene sheet was constructed with help of the function `graphene_nanoribbon` in ASE. As in the coronene case the cell height was set to 20 Å and the graphene sheet was placed at a height of 5 Å. The graphene cell contained 24 carbon atoms giving resulting side lengths of 8.52 Å $\times$ 7.37853644 Å in the planar directions. One cell of graphene with a hydrogen atom adsorbed at the Top position can be seen in figure 3.7.

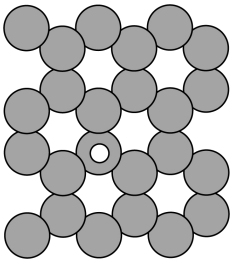

Figure 3.7: One cell of graphene used in calculations. Here a hydrogen atom is adsorbed at the Top site.

**Versions and parameters**

The H - graphene system was built using ASE 3.4.1.1861. The energies for vdW-DF1 and vdW-DF2 were calculated in a non-self consistent way based on revPBE, see section 2.3.5. The calculator grid-spacing was specified as `h = 0.18`, the eigensolver was set to `rmm-diis` and the convergence criteria `total energy change` was set to $10^{-6}$ eV/atom. The number of k-points were 8 in periodic directions parallel to the plane and 1 in the non periodic direction perpendicular to the plane giving a total of 64 k-points. For this system all calculations were performed using GPAW development build r7883.

### 3.4.4 The $H_2$ - Coronene system

This system was set up very similar to the H - Coronene system described in section 3.4.2, but with a $H_2$ molecule instead of a single hydrogen atom. The cell size and bond lengths were the same as in the hydrogen case. The system can be seen in figure 3.8.

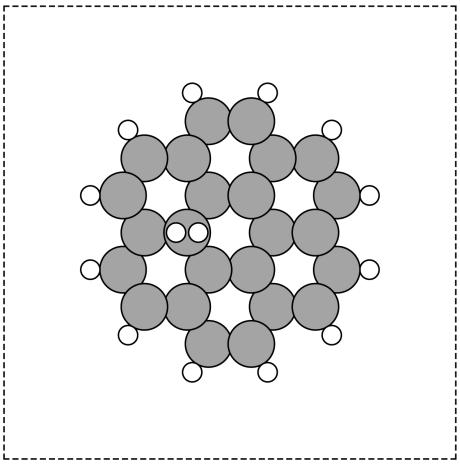

Figure 3.8: The cell with coronene used in calculations. Here a hydrogen molecule is adsorbed at the Top site. The direction of the molecule axis was the same also for placement at the Bridge and Hollow sites on coronene.

**Versions and parameters**

The $H_2$ - coronene system was built using ASE 3.4.1.1765. The energies for vdW-DF1 and vdW-DF2 were calculated in a non-self consistent way based on revPBE, see section 2.3.5. The underlying self consistent revPBE calculation was a spin-polarised calculation performed using GPAW 0.7.2.6974. The calculator grid-spacing was specified as `h = 0.18`, the `eigensolver` was set to `cg` and convergence criteria `total energy change` was set to $10^{-6}$ eV/atom. The non-self consistent vdW-DF1 calculation was performed using GPAW 0.7.2.6974. The non-self consistent vdW-DF2 calculation was performed using GPAW development build r7883.

### 3.4.5 The $H_2$ - Graphene system

This system was set up very similar to the H - Graphene system described in section 3.4.3, but with a $H_2$ molecule instead of a single hydrogen atom. The cell size and bond lengths were the same as for H - graphene. The adsorbed molecule can be seen in figure 3.9.

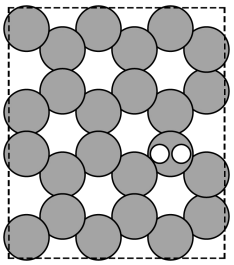

Figure 3.9: One cell of graphene used in calculations. Here a hydrogen molecule is adsorbed at the Top site. The direction of the molecule axis was the same also for placement at the Bridge and Hollow sites on graphene.

#### Versions and parameters

The $H_2$ - graphene system was built using ASE 3.4.1.1861. The energies for vdW-DF1 and vdW-DF2 were calculated in a non-self consistent way based on revPBE, see section 2.3.5. For this system all calculations were performed using GPAW development build r7883. The number of k-points were 8 in periodic directions parallel to the plane and 1 in the non periodic direction perpendicular to the plane giving a total of 64 k-points.

# Chapter 4

# Results and discussion

In this chapter the results of the calculations carried out in this work are presented. The results are discussed in the context of related studies. Binding energies are always calculated as the difference between total energies for the system under investigation and reference values, see section 3.3.

## 4.1 Chemisorption energies

Calculations with atomic hydrogen above unrelaxed coronene (figure 3.3) along with other studies (e.g. [4]) indicate that H can chemisorb at the Top site but not at the Bridge or Hollow sites. To compare different surface models the chemisorption well was calculated for hydrogen at the Top site above coronene, relaxed coronene and graphene. The resulting three curves can be seen in figure 4.1(a). The extreme values for the chemisorption are summarised in table 4.1. No chemisorption well was found for molecular hydrogen $H_2$.

Table 4.1: Chemisorption results for hydrogen at the Top site. The numbers for vdW-DF1 and vdW-DF2 are from non-self consistent calculations based on underlying self consistent revPBE (GGA) calculations.

| System | revPBE | | vdW-DF1 | | vdW-DF2 | |
|---|---|---|---|---|---|---|
| | E [meV] | d [Å] | E [meV] | d [Å] | E [meV] | d [Å] |
| H - Coronene | 155 | 1.2 | 15 | 1.25 | 3 | 1.25 |
| H - Cor w/relax | 361 | 1.5 | 542 | 1.5 | 488 | 1.5 |
| H - Graphene | 567 | 1.2 | 347 | 1.2 | 294 | 1.2 |

### 4.1.1 Relaxation of a surface carbon atom

From figure 4.1(a) and table 4.1 it is clear that the chemisorption well for the H-coronene system changes if relaxation of the closest surface carbon atom is allowed. This behaviour is in agreement with the calculations performed by Jeloica and Sidis [4]. The relaxation process was done with revPBE and the values for vdW-DF1 and vdW-DF2 were calculated in a non self-consistent

way. At the chemisorption minimum the hydrogen atom was positioned 1.5 Å above the coronene plane, and the closest carbon atom moved 0.36 Å towards the hydrogen atom. No calculations including relaxation was performed for graphene.

## 4.2 The barrier between the wells

There is a barrier between the physisorption well and the chemisorption well for all three surface models; coronene, relaxed coronene and graphene. The barriers are visible in figure 4.1(a) and the barrier heights are summarised in table 4.2.

The relaxed coronene calculations show a barrier around 200 meV, which is in good agreement with earlier studies summarised in [16]. In the case of spin-polarised H-graphene calculations the barrier seems to be much higher, up to 597 meV. However, this number is preliminary in the sense that I have not included atomic relaxations. I expect that inclusion of the morphology changes which arise in and near the chemisorption region will significantly lower this barrier.

The barrier region is where the system changes from a spin-paired (total magnetic moment = 0) to a spin-polarised (total magnetic moment = 1) state. The degree of spin-polarisation as a function of separation distance can be seen in figure 4.5(b). In the physisorption region (to the right of the barrier) the system is almost fully spin-polarised. In the chemisorption region (to the left of the barrier) the system is spin-paired, i.e. the total magnetic moment is 0. Since the system is partially spin-polarised in the barrier region it is important to use spin-polarised calculations to get accurate results.

Table 4.2: Barrier heights between the chemisorption and physisorption wells for hydrogen at the Top site. The numbers for vdW-DF1 and vdW-DF2 are from non-self consistent calculations based on revPBE. The barrier height is calculated relative to the bottom of the physisorption well. The results for revPBE are given relative to the energy at an infinite separation distance because there is no physisorption well with GGA (and in particular revPBE) calculations.

| System | revPBE [meV] | vdW-DF1 [meV] | vdW-DF2 [meV] |
|---|---|---|---|
| H - Coronene | 555 | 472 | 525 |
| H - Cor w/relax | 337 | 214 | 228 |
| H - Graphene | 824 | 508 | 597 |

## 4.3 Physisorption energies

The standard GGA functional revPBE does not show any physisorption well for H or $H_2$. When dispersion forces are included in the model (as in vdW-DF and vdW-DF2) there is a clear physisorption well for both H and $H_2$. This qualitative behaviour is in agreement with other studies including van der Waals forces described in section 1.3.

The physisorption energy varies less than 10 meV for H when comparing three different adsorption sites (figure 4.2(b)). Site independence is also supported by the calculations performed over a coronene molecule (figure 4.4(a)) where the adsorption energy varies very little inside the central benzene ring.

Since the physisorption energies are about the same for H and $H_2$, and H-atoms seem to be mobile on the surface, this indicate a possibility of forming molecular hydrogen on the graphitic surface via the Langmuir-Hinshelwood mechanism (see section 1.1.2). However, all results in this thesis are valid at temperature 0 and although the interstellar medium is cold it is possible that even small temperatures might cause atoms to desorb from the surface before they form $H_2$. To investigate the actual formation rates the binding energies computed in this thesis could be used to calculate probabilities for adsorption and desorption. A thermodynamic rate equation based on these probabilities can yield formation rates for $H_2$ that could be compared to experiments and observations, but this is beyond the scope of this thesis.

### 4.3.1 $H_2$ above a surface

As expected there is no chemisorption well for $H_2$, but there is a physisorption well around 3 Å. The binding energy for $H_2$ on a graphitic surface is around 60 meV which is about 10 meV less than for atomic hydrogen. The extreme values for the physisorption well are summarised in table 4.3.

Table 4.3: Non self-consistent calculations based on revPBE for molecular hydrogen above a graphitic surface.

| System | Site | vdW-DF1 | | vdW-DF2 | |
|---|---|---|---|---|---|
| | | E [meV] | d [Å] | E [meV] | d [Å] |
| $H_2$ - Coronene | Hollow | 71 | 3.25 | 59 | 3.0 |
| $H_2$ - Graphene | Hollow | 75 | 3.25 | 61 | 3.0 |

In the case of unrelaxed coronene the physisorption energy was calculated for the Top, Bridge and Hollow sites. The graphs for all three sites can be seen in figure 4.2(a). The preferred adsorption site was Hollow (E = 59 meV), second preferred site was Bridge (E = 51 meV) and the least preferred site was Top (E = 50 meV).

In the case of graphene the physisorption energy was also calculated for the Top, Bridge and Hollow sites. The preferred adsorption site was Hollow (E = 61 meV), second preferred site was Bridge (E =53 meV) and the least preferred site was Top (E = 52 meV).

### 4.3.2 H above a surface

The physisorption well was calculated for three different surface models: coronene, relaxed coronene and graphene. The three resulting binding energy graphs can be seen in figure 4.3. The extreme values for the physisorption well are summarised in table 4.4.

In the case of unrelaxed coronene the physisorption energy was also calculated for the Hollow and Bridge sites. The graphs for all three sites can be seen

Table 4.4: Physisorption results for atomic hydrogen. Non self-consistent calculations based on revPBE. For unrelaxed coronene where all three sites were compared the Hollow adsorption energy was always lowest. Therefore the Hollow site values are presented here for unrelaxed coronene. For relaxed coronene and graphene only the values for the top site were calculated and therefore these are shown here.

| System | Site | vdW-DF1 | | vdW-DF2 | |
|---|---|---|---|---|---|
| | | E [meV] | d [Å] | E [meV] | d [Å] |
| H - Coronene | Hollow | 73 | 3.0 | 70 | 2.85 |
| H - Coronene w/relax | Top | 69 | 3.0 | 68 | 2.85 |
| H - Graphene | Top | 76 | 3.0 | 70 | 3.0 |

in figure 4.2(b). The preferred adsorption site was Hollow (E =70 meV), second preferred site was Bridge (E =68 meV) and the least preferred site was Top (E =67 meV).

### A surface plot of the binding energy

To further investigate the coronene physisorption site independence the binding energy was also calculated at 1600 different points on a regular grid over the coronene molecule. The grid covered a square area of $10 \times 10 = 100\,\text{Å}^2$ around the centre point of the coronene molecule. The binding energy was calculated at each point when the hydrogen atom was positioned 2.85 Å over the coronene plane. This distance was chosen since the three sites in figure 4.2(b) all have a minimum at 2.85 Å. The resulting surface plot can be seen in figure 4.4(a). The surface plot indicates that the physisorption of atomic hydrogen on coronene is essentially site independent provided the adsorption site is close to the central carbon ring.

### Comparison with other studies

Table 4.5 shows a comparison of calculations for atomic hydrogen on coronene: accurate quantum chemical MP2 calculations by Bonfanti et al [12], calculations by Jie Ma et al [18] and calculations performed in this thesis work. Table 4.6 shows a comparison for atomic hydrogen on graphene: an experiment by Ghio et al [10], Jie Ma et al [18] and results from this thesis work. MP2 calculations are considered very accurate but cannot be used for infinite systems like graphene. Diffusion MonteCarlo (DMC) calculations are also considered to be good, but clearly cannot handle the graphene system. Density functional theory using vdW-DF1 and vdW-DF2 works for both finite and infinite systems, but overestimates the binding energy by almost a factor of two. This is when comparing to MP2 calculations (for coronene) and an experiment for graphite. The fact that the results are close for vdW-DF1 calculations performed by Jie Ma et al [18] and in this thesis suggests that vdW-DF1 calculations work equally well in the softwares VASP and GPAW. Unfortunately [18] do not present any values for the chemisorption or barrier regions.

Table 4.5: Comparison of physisorption results for atomic hydrogen on coronene.

| Method | Binding energy [meV] | Binding distance [Å] |
|---|---|---|
| Quantum chemical MP2 [12] | 39.5 | 2.93 |
| Diffusion Monte Carlo (DMC) [18] | 26 | 2.95 |
| vdW-DF1 (VASP) [18] | 75 | 2.99 |
| vdW-DF1 (GPAW) [This work] | 73 | 3.0 |
| vdW-DF2 (GPAW) [This work] | 70 | 2.85 |

Table 4.6: Comparison of physisorption results for atomic hydrogen on graphene. The values for Diffusion Monte Carlo are in parenthesis because the authors express doubt about the validity of these numbers.

| Method | Binding energy [meV] | Binding distance [Å] |
|---|---|---|
| Experiment for graphite [10] | 39.2 | - |
| Diffusion Monte Carlo (DMC) [18] | (5) | (3) |
| vdW-DF1 (VASP) [18] | 81 | 3.0 |
| vdW-DF1 (GPAW) [This work] | 76 | 3.0 |
| vdW-DF2 (GPAW) [This work] | 70 | 3.0 |

## 4.4 Coronene as a model of graphene

In the physisorption region there is very small difference between coronene and graphene results, see tables 4.4 and 4.3. This suggests that coronene is a good model for physisorption on a graphitic surface and can be used to obtain physisorption energies for both H and $H_2$ (and possibly also other small molecules). Figure 4.4(a) implies that the coronene molecule is a good model for physisorption on a graphitic surface only locally in the region close to the central carbon ring. For computational investigations where a larger surface area is required it is therefore important to either use a larger coronene-like molecule, or preferably a periodic graphene or graphite surface.

Since the binding energy might change a lot in the chemisorption region if relaxation is allowed (see figure 4.1(a) for relaxed coronene) it is not possible to conclude whether or not coronene is a good model or not for graphene in the chemisorption region. The relaxation performed for coronene in this thesis was limited only to one carbon atom and was only performed for hydrogen on coronene. To get a more complete picture of the relation between coronene and graphene in the chemisorption region relaxation must also be done for hydrogen above graphene, and the relaxation must include more carbon atoms. Including more atoms is important because it is unnatural to alter just one atom in an infinite graphene sheet.

## 4.5 Spin-paired vs spin-polarised calculations

The free hydrogen atom is spin-polarised in its ground state since it has only 1 electron and will therefore have a total magnetic moment of 1. When hydrogen interacts with other atoms it is possible that the total system will have a different magnetic moment. To investigate this behaviour both spin-paired and spin-polarised calculations were done for the system atomic hydrogen at the Top site above a graphene surface. The resulting binding energy curves can be seen in figure 4.5(a).

The curve called *Spin-polarised* is the result of doing a spin-polarised calculation i.e. allowing the system to change its magnetic moment. This is the curve used to obtain the binding energies for atomic hydrogen on graphene presented in this thesis. The curve called *Spin-paired* is the result of doing the same calculation in a spin-paired way, i.e. forcing the total magnetic moment to be zero.

It might seem strange that that the spin-paired curve does not approach zero as the separation distance becomes large. But, this is not surprising because the reference energy is taken to be the spin-polarised hydrogen atom and not a spin-paired hydrogen atom. Since the spin-paired system will never be able to reach the energy of the spin-polarised reference state, there will be an offset even at an infinite separation distance.

The calculations suggest that atomic hydrogen can form a strong chemical bond close to the graphene surface at a distance between 1 Å and 1.5 Å, see figure 4.1(a). As can be seen in figure 4.5(b) the system is spin-paired in the chemisorption region (to the left of the barrier), i.e. the total magnetic moment is 0. This is physically meaningful since a strong chemical bond means a charge rearrangement which also enables pairing of electrons. Here one expect a spin-paired calculation to give the same result as a spin-polarised calculation (provided that one uses the same reference). It is clear that the curves in figure 4.5(a) indeed do give the same result in the chemisorption region.

In the barrier region around 2 Å the system is in a mixed state with a magnetic moment shifting from 0 to 1 as visible in figure 4.5(b). In this region it is hard to make the calculations converge. High convergence thresholds and small mixing parameters are required compared to other separation distances.

In the physisorption well and at larger separation distances the system is spin-polarised with a total magnetic moment of 1. It is interesting to see that the system is indeed spin-polarised in the physisorption region which indicates that binding in this region is not due to a charge rearrangement.

As a final remark about spin polarisation I again want to discuss the vdW-DF1 calculations of Jie Ma et. al [18]. In this article the PAW method is used through the implementation VASP to calculate vdW-DF1 binding energies. Jie Ma et. al writes that *spin-polarised calculations are used* in their DFT calculations. However, they do not provide any reference to a spin-polarised derivation of the van der Waals density functional. It is possible that spin polarised vdW-DF1 calculations are implemented the same way in VASP as in GPAW. Although it is possible to use the assumption of a spin-independent kernel (described in section 2.4.1) it is important to emphasise that at the moment there exists *no* true extension of vdW-DF for spin-polarised cases. A derivation built upon a fully spin-dependent van der Waals density functional theory would certainly be appreciated if published.

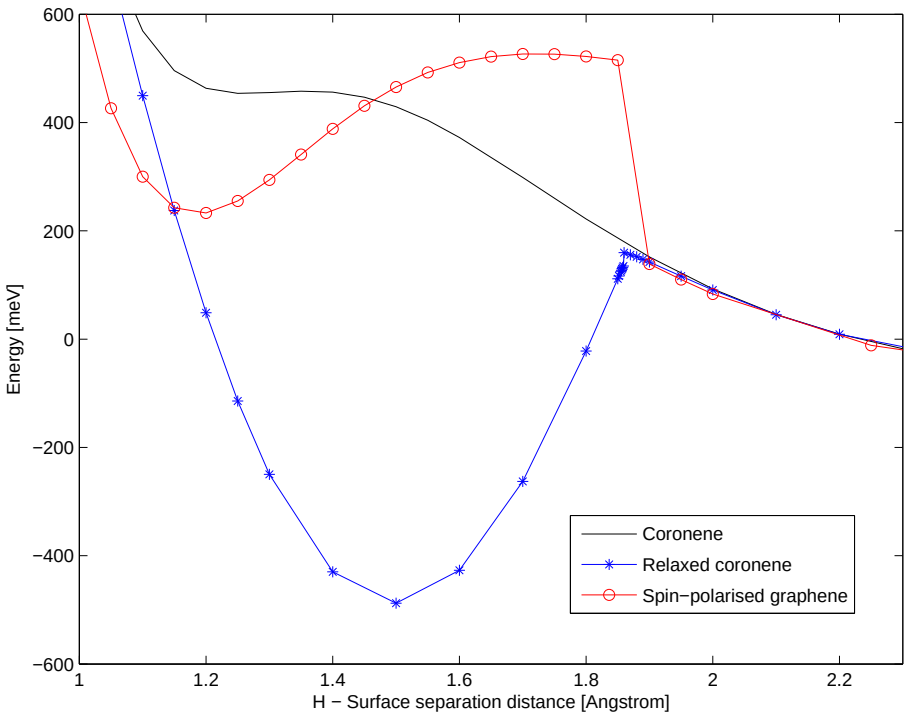


(a) The chemisorption and barrier regions for atomic hydrogen above three surfaces.

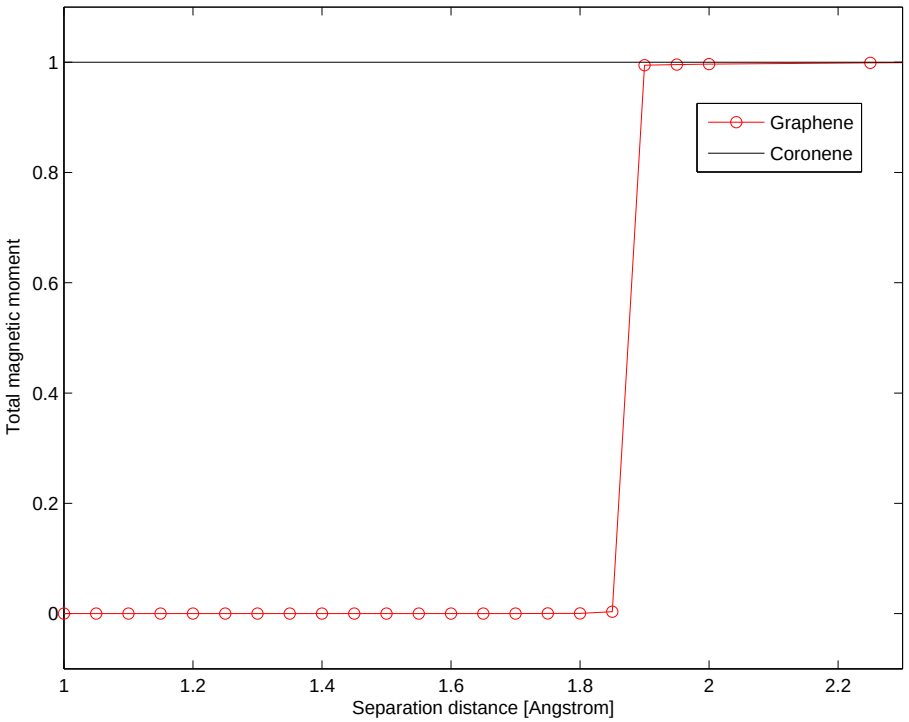


(b) Total magnetic moment for atomic hydrogen above graphene and coronene.

Figure 4.1: Atomic hydrogen adsorbed on three surfaces. Panel (a) shows the binding energy as a function of separation distance for a single hydrogen atom over three different surfaces: coronene, relaxed coronene and graphene. The hydrogen atom is positioned at the top site in all three cases. These are non-self consistent vdW-DF2 calculations based on revPBE. In the barrier region the system changes from a spin-paired to a spin-polarised state, see also panel (b) and figure 4.5(a). Panel (b) shows the magnitude of the total magnetic moment for a single hydrogen atom over both coronene and graphene as a function of separation distance.

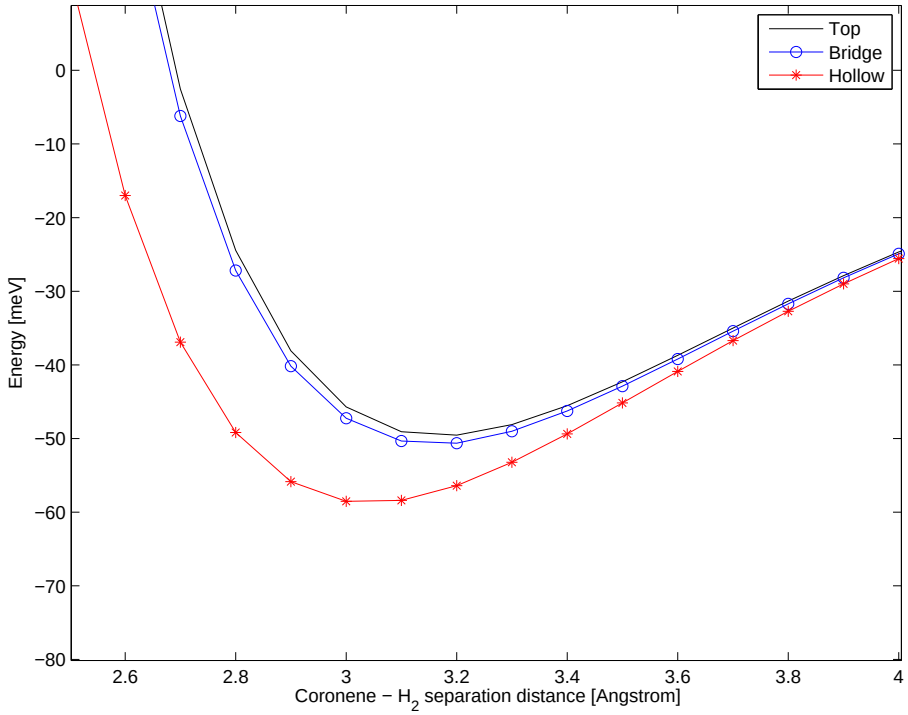


(a) The physisorption well for $H_2$ above coronene.

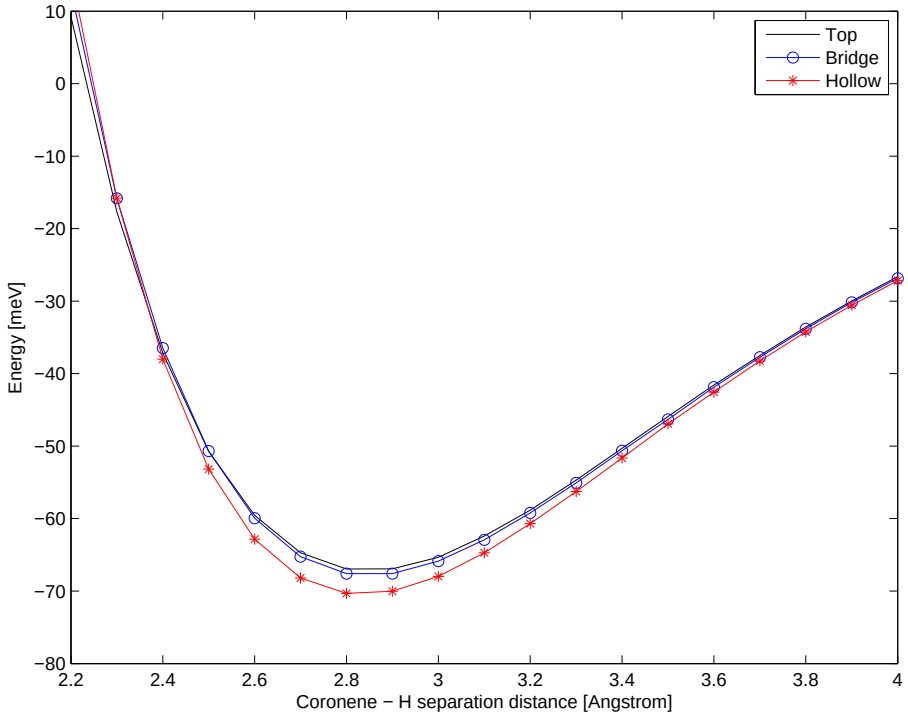


(b) The physisorption well for H above coronene.

Figure 4.2: Non-self consistent vdW-DF2 calculations based on revPBE for H and $H_2$. Panel (a) shows the physisorption well for $H_2$ over a coronene molecule surface for three different sites. Panel (b) shows the physisorption well for a single hydrogen atom over a coronene molecule surface for three different sites.

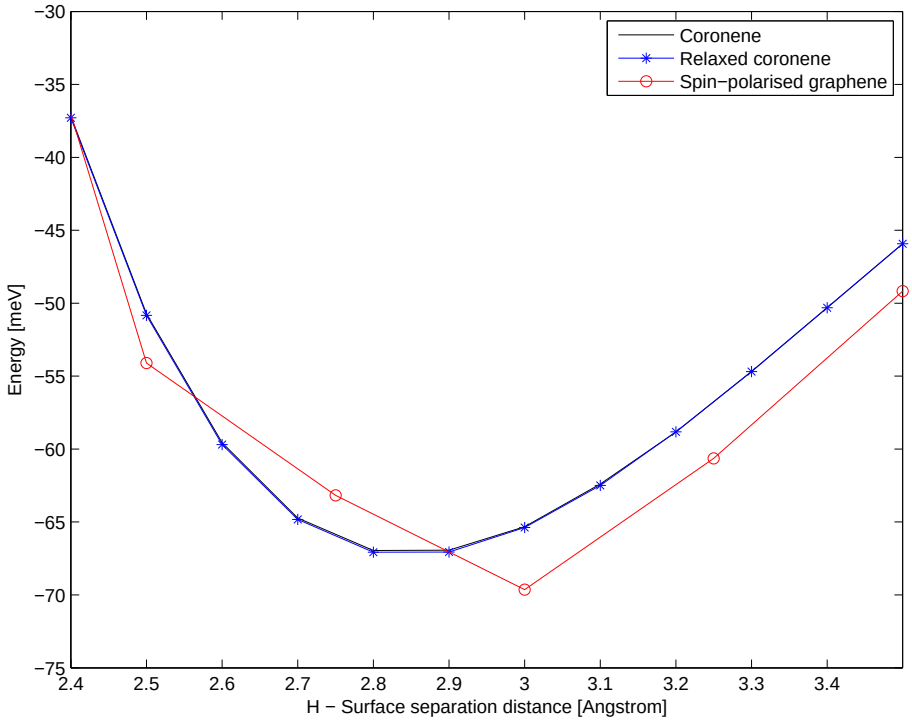


Figure 4.3: The physisorption well for a single hydrogen atom over a surface for three different surfaces. Non-self consistent vdW-DF2 calculations based on revPBE. The hydrogen atom is positioned at the top site in all three cases. The curves for unrelaxed coronene and relaxed coronene are almost identical.

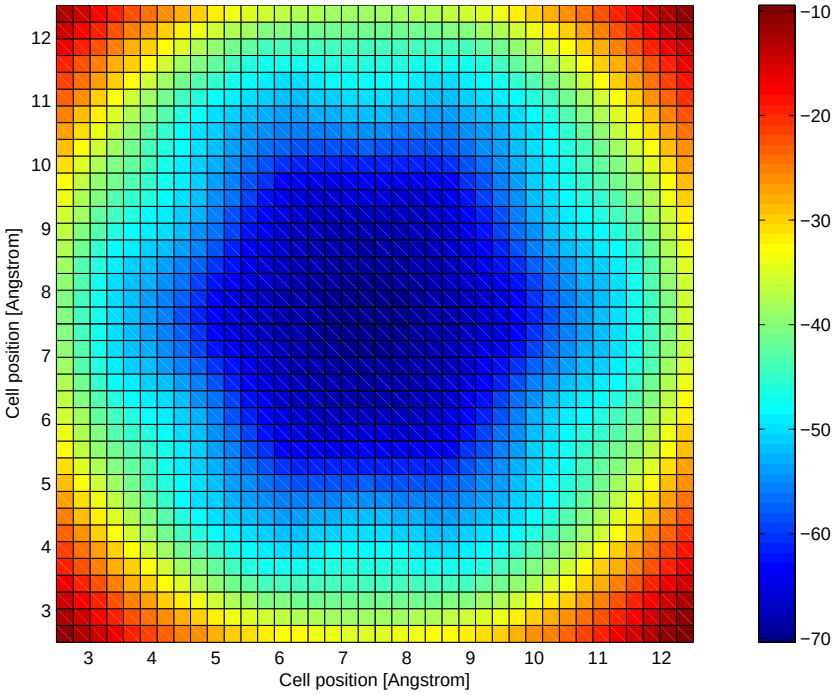


(a) Binding energy of H adsorbed on coronene.

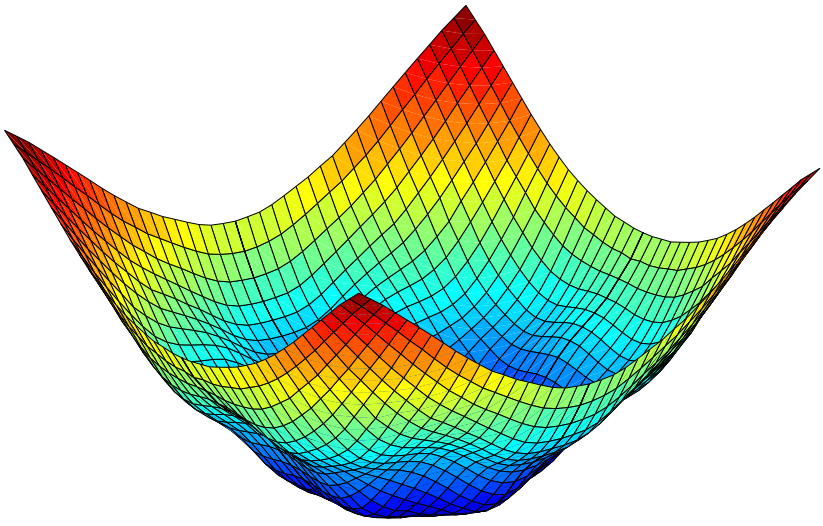

(b) Surf (3D) version of figure (a).

Figure 4.4: Atomic hydrogen adsorbed above a coronene molecule. Panel (a) shows the binding energy (in meV, see colorbar) calculated on a 1600 points grid over a square area of 100 $Å^2$ covering the coronene molecule. The binding energy was calculated at each point when the hydrogen atom was positioned 2.85 Å over the coronene plane. The six outer hollows (rings) in the coronene molecule is clearly visible. The innermost hollow ring is in the centre. Panel (b) shows a surf (3D) version of panel (a).

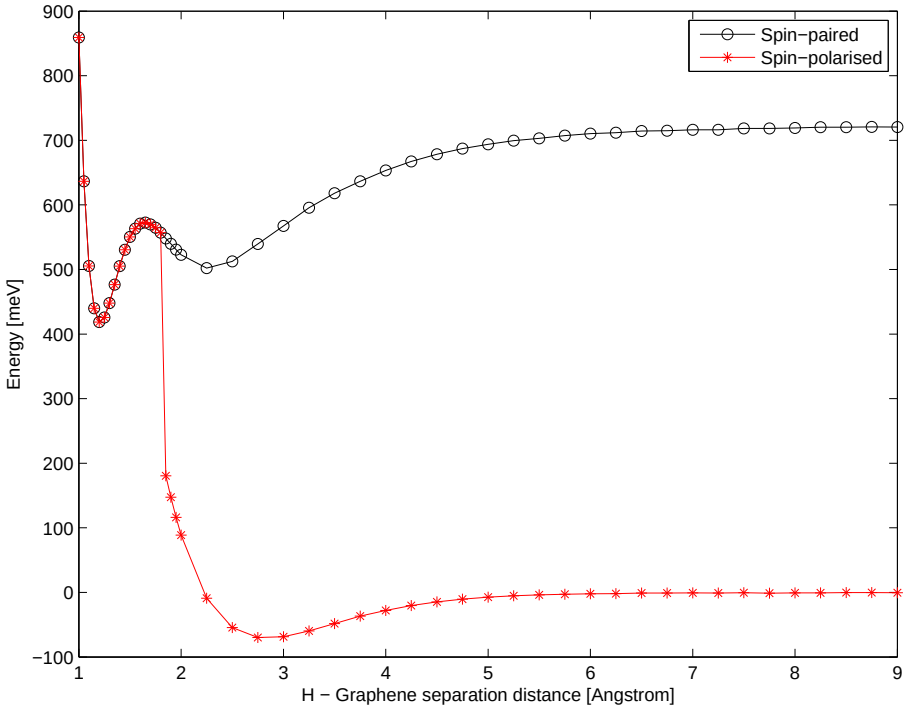


(a) Comparison of spin-polarised and spin-paired calculations.

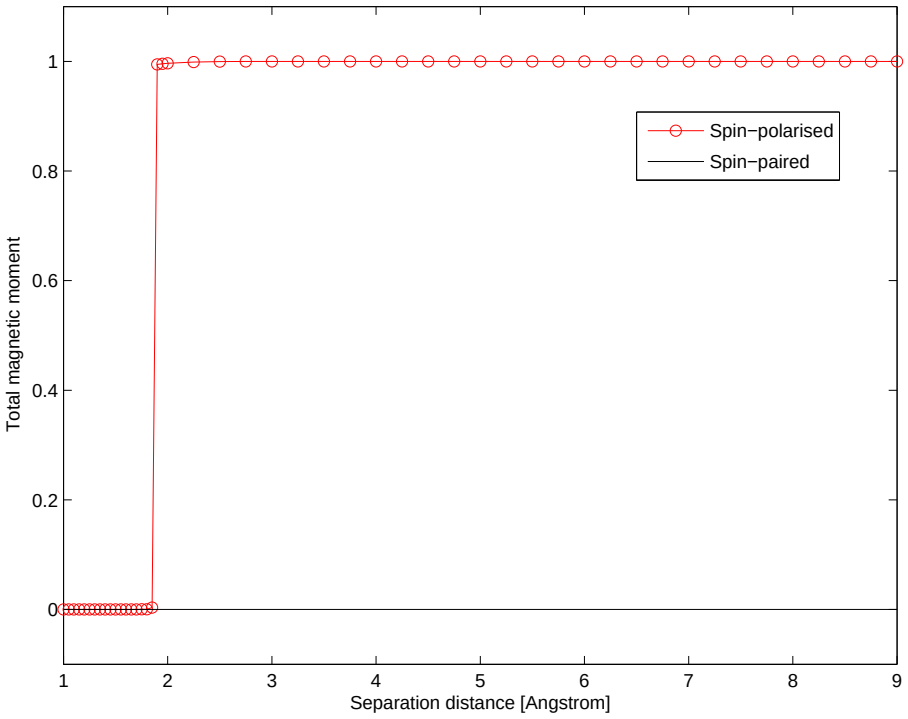


(b) Total magnetic moment for H on graphene.

Figure 4.5: A comparison between spin-paired and spin-polarised calculations for atomic hydrogen above graphene. Panel (a) shows the binding energy from both a spin-paired and a spin-polarised calculation for atomic hydrogen adsorbed at the Top site above graphene. These are both non-self consistent vdW-DF2 calculations based on revPBE. In the barrier region the system changes from a spin-paired to a spin-polarised state, see also figure 4.5(a). Panel (b) shows the magnitude of the total magnetic moment for a single hydrogen atom over a graphene surface as a function of separation distance. This data is taken from the calculations presented in panel (a).

# Chapter 5

# Summary and outlook

The functionals vdW-DF1 and vdW-DF2 do describe dispersive forces behind physisorption in a better way than the traditional GGA functional revPBE. However both vdW-DF1 and vdW-DF2 overestimates the physisorption energy by almost a factor of 2 compared to experiment and accurate quantum chemical calculations. The results in this thesis predict a physisorption energy for atomic hydrogen on a graphitic surface of 70 meV whereas experiment and accurate quantum chemical (MP2) calculations predict a physisorption energy of $\approx$40 meV.

The molecule coronene seems to be a good model of a graphene surface in the case of hydrogen physisorption, provided that the physisorption site is inside (or close to) the middle carbon-ring.

Calculations with vdW-DF1 and vdW-DF2 predict that hydrogen can bind to a graphitic surface both through chemisorption and physisorption, and that there is a barrier between these two wells. Physisorption of atomic hydrogen on a graphitic surface seems to be essentially site independent with changes in binding energy less than 10 meV for atoms moving around on the surface. A site-independent physisorption is consistent with other related computational studies.

The results also suggest that it is important to do spin-polarised calculations when investigating atomic hydrogen above a graphitic surface. This is partly because a single hydrogen atom cannot be described correctly within spin-paired DFT, but also because the atomic hydrogen - graphene system is partially polarised in the barrier region.

There are several interesting ways to extend the work done in this thesis. One way is to learn more about convergence and mixing in GPAW and redo the calculations in this thesis using *self-consistent* vdW-DF1 and vdW-DF2. It would be interesting to see if the difference actually is small also for these systems compared to the results presented in this thesis.

It would also be interesting to do another calculation for H on graphene where the closest carbon atom would be allowed to relax similarly to what has been done for H on coronene in this thesis.

At the moment there exists no spin-dependent derivation of the van der Waals density functional method. A derivation built upon a fully spin-dependent van der Waals density functional theory would be valuable for anyone interested in describing systems where both van der Waals forces and spin-polarisation play an important role.

# Bibliography


[1] A. G. G. M. Thielens. *The physics and Chemistry of the Interstellar Medium*. Cambridge University Press, 2010.

[2] Koichi Momma and Fujio Izumi. *VESTA*: a three-dimensional visualization system for electronic and structural analysis. *Journal of Applied Crystallography*, 41(3):653–658, Jun 2008.

[3] Kellar Autumn, Metin Sitti, Yiching A. Liang, Anne M. Peattie, Wendy R. Hansen, Simon Sponberg, Thomas W. Kenny, Ronald Fearing, Jacob N. Israelachvili, and Robert J. Full. Evidence for van der waals adhesion in gecko setae. *Proceedings of the National Academy of Sciences*, 99(19):12252–12256, 2002.

[4] L Jeloaica and V Sidis. Dft investigation of the adsorption of atomic hydrogen on a cluster-model graphite surface. *Chemical Physics Letters*, 300:157–162, January 1999.

[5] N. Jacobson, B. Tegner, E. Schröder, P. Hyldgaard, and B. Lundqvist. Hydrogen dynamics in magnesium and graphite. *Computational materials science*, 24:273–277, 2002.

[6] M. Dion, H. Rydberg, E. Schröder, D. C. Langreth, and B. I. Lundqvist. Van der waals density functional for general geometries. *Phys. Rev. Lett.*, 92(24):246401, Jun 2004.

[7] D C Langreth, B I Lundqvist, S D Chakarova-Käck, V R Cooper, M Dion, P Hyldgaard, A Kelkkanen, J Kleis, Lingzhu Kong, Shen Li, P G Moses, E Murray, A Puzder, H Rydberg, E Schröder, and T Thonhauser. A density functional for sparse matter. *Journal of Physics: Condensed Matter*, 21(8):084203, 2009.

[8] Johannes D. van der Waals. The equation of state for gases and liquids. Nobel Lecture, December 12 1910.

[9] Charles Kittel. *Introduction to solid state physics*. John Wiley and Sons, Inc., 2005.

[10] E Ghio, L Mattera, C Salvo, F Tommasini, and U Valbusa. Vibrational spectrum of h and d on the (001) graphite surface from scattering experiments. *Chemical Physics*, 73:556–561, 1980.

[11] Xianwei Sha and Bret Jackson. First-principles study of the structural and energetic properties of h atoms on a graphite (0 0 0 1) surface. *Surface Science*, 496(3):318 – 330, 2002.

[12] Matteo Bonfanti, Rocco Martinazzo, Gian Franco Tantardini, and Alessandro Ponti. Physisorption and diffusion of hydrogen atoms on graphite from correlated calculations on the h-coronene model system. *Physical Chemistry Letters*, 111:5825–5829, 2007.

[13] George M. Psofogiannakis and George E. Froudakis. Dft study of the hydrogen spillover mechanism on pt-doped graphite. *The Journal of Physical Chemistry C*, 113(33):14908–14915, 2009.

[14] Stefan Grimme. Accurate description of van der waals complexes by density functional theory including empirical corrections. *Journal of Computational Chemistry*, 25(12):1463–1473, 2004.

[15] Stefan Grimme. Semiempirical gga-type density functional constructed with a long-range dispersion correction. *Journal of Computational Chemistry*, 27(15):1787–1799, 2006.

[16] Richardo M Ferullo, Nicolás F Domancich, and Norberto J Castellani. On the performance of van der waals corrected-density functional theory in describing the atomic hydrogen on graphite. *Chemical Physics Letters*, 500:283–286, 2010.

[17] Yue Wang and John P. Perdew. Correlation hole of the spin-polarized electron gas, with exact small-wave-vector and high-density scaling. *Phys. Rev. B*, 44(24):13298–13307, Dec 1991.

[18] Jie Ma, Angelos Michaelides, and Dario Alfè. Binding of hydrogen on benzene, coronene, and graphene from quantum monte carlo calculations. *Chemical Physics*, 134:134701, 2011.

[19] Alexander L. Fetter and John Dirk Walecka. *Quantum theory of many-particle systems*. McGraw-Hill, Inc., 1971.

[20] P. Hohenberg and W. Kohn. Inhomogeneous electron gas. *Phys. Rev.*, 136(3B):B864–B871, Nov 1964.

[21] Richard M. Martin. *Electronic structure: basic theory and practical methods*. Cambridge University Press, 2010.

[22] W. Kohn and L. J. Sham. Self-consistent equations including exchange and correlation effects. *Phys. Rev.*, 140(4A):A1133–A1138, Nov 1965.

[23] Peter E Blöchl. Projector augmented-wave method. *Phys. Rev. B*, 50(24):17953–17979, Dec 1994.

[24] Ask Hjort Larsen. Localized atomic orbital basis sets in the projector augmented wave method. Master's thesis, Center for Atomic-scale Materials Design, Department of Physics, Technical University of Denmark, June 2008.

[25] Yingkai Zhang and Weitao Yang. Comment on "generalized gradient approximation made simple". *Phys. Rev. Lett.*, 80(4):890, Jan 1998.

[26] T. Thonhauser, Valentino R. Cooper, Shen Li, Aaron Puzder, Per Hyldgaard, and David C. Langreth. Van der waals density functional: Self-consistent potential and the nature of the van der waals bond. *Phys. Rev. B*, 76(12):125112, Sep 2007.

[27] Kristian Berland. Bound by long-range interactions: Molecular crystals and benzene on cu(111). licentiate thesis, chalmers university of technology, 2009.

[28] Kyuho Lee, Éamonn D. Murray, Lingzhu Kong, Bengt I. Lundqvist, and David C. Langreth. Higher-accuracy van der waals density functional. *Phys. Rev. B*, 82(8):081101, Aug 2010.

[29] T. Thonhauser, Per Hyldgaard, and B. I. Lundqvist. Personal communication, April 2011.

[30] C3SE website: http://www.c3se.chalmers.se. Hardware beda, 2011-05-01.

[31] J. J. Mortensen, L. B. Hansen, and K. W. Jacobsen. Real-space grid implementation of the projector augmented wave method. *Phys. Rev. B*, 71(3):035109, Jan 2005.

[32] J Enkovaara, C Rostgaard, J J Mortensen, J Chen, M Dułak, L Ferrighi, J Gavnholt, C Glinsvad, V Haikola, H A Hansen, H H Kristoffersen, M Kuisma, A H Larsen, L Lehtovaara, M Ljungberg, O Lopez-Acevedo, P G Moses, J Ojanen, T Olsen, V Petzold, N A Romero, J Stausholm-Møller, M Strange, G A Tritsaris, M Vanin, M Walter, B Hammer, H Häkkinen, G K H Madsen, R M Nieminen, J K Nørskov, M Puska, T T Rantala, J Schiøtz, K S Thygesen, and K W Jacobsen. Electronic structure calculations with gpaw: a real-space implementation of the projector augmented-wave method. *Journal of Physics: Condensed Matter*, 22(25):253202, 2010.

[33] S. R. Bahn and K. W. Jacobsen. An object-oriented scripting interface to a legacy electronic structure code. *Comput. Sci. Eng.*, 4(3):56–66, MAY-JUN 2002.